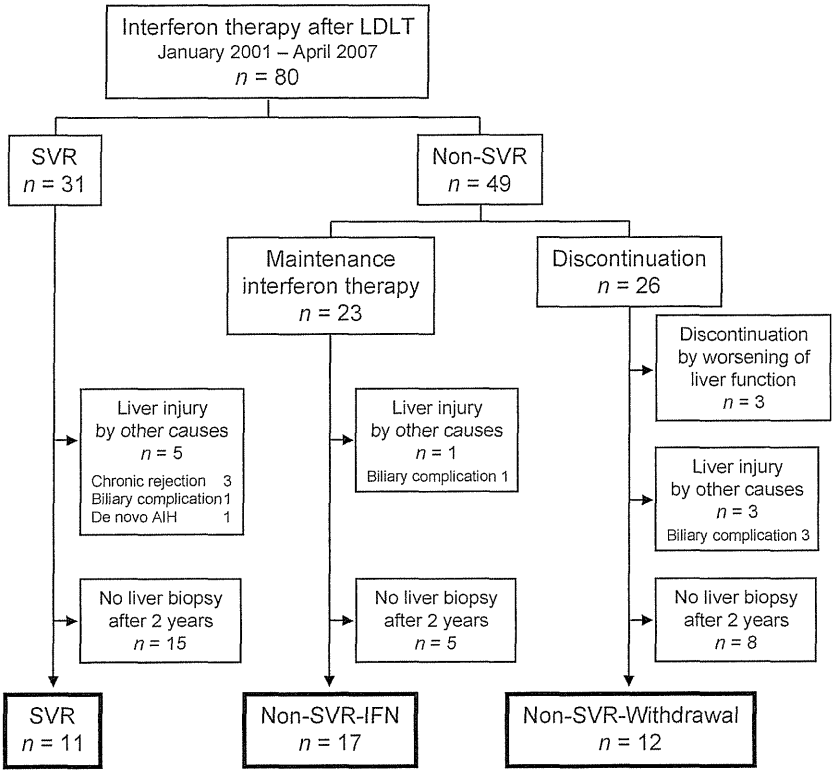

Fig. 1 Flow diagram showing the outcome of interferon therapy for patients with recurrent hepatitis C after living donor liver transplantation and indicating the classification of patients in this study.

23 (47%) received the low-dose peginterferon maintenance therapy, while 26 (53%) discontinued treatment within 12 months and did not receive low-dose peginterferon maintenance therapy as this was the patients' wish (n = 4), because of general fatigue (n = 4), recurrent hepatocellular carcinoma (n = 4), worsening of liver function (n = 3), biliary complications (n = 3), heart failure (n = 2), brain haemorrhage (n = 1), dementia (n = 1), sinusitis (n = 1), anaemia (n = 1), neutropenia (n = 1), and haemosputum (n = 1).

Of the 31 SVR patients, five were excluded because of chronic rejection (n = 3), biliary complications (n = 1) and *de novo* AIH (n = 1). Fifteen patients did not have liver biopsies more than 2 years after the initiation of the interferon therapy, mainly because liver function tests were normal. The remaining 11 patients were classified as the SVR group for analysis in this study. Among the 23 patients who received maintenance therapy, one patient with biliary complications and five patients who did not have liver biopsy more than 2 years after the initiation of therapy were excluded from the study. The remaining 17 patients were classified into the non-SVR-IFN group. Among the 26 patients who discontinued treatment within 12 months, three patients who initially experienced worsening of liver function were excluded because of the rapid progression of HCV; an additional three patients were excluded because of biliary complications. Eight patients were excluded because they had no liver biopsies taken more than 2 years after the initiation of the treatment. The remaining 12 patients were classified into the non-SVR-Withdrawal group. Cumulatively, we analysed the long-term histological changes of 40 patients: 11 in the SVR group (27.5% of the total), 17 in the non-SVR-IFN group (42.5% of the total) and 12 in the non-SVR-Withdrawal group (30% of the total).

There were no significant differences in the baseline characteristics among patients in the SVR, non-SVR-IFN, and non-SVR-Withdrawal groups (Table 1). The median age of patients at the beginning of therapy was 56.5 years (range, 15–70 years). The treatment started at a median of 9.5 months (range, 1.1–85.3 months) after LDLT. Thirty-five patients (88%) were infected with HCV genotype 1b. HCV genotypes of the remaining patients were 2a (n = 3), 2b (n = 1) and undetermined (n = 1). Median serum HCV RNA load was 2290 kIU/mL (range, 73.7–5000 kIU/mL); i.e. most patients had an extremely high viral load. Before the treatment, the necroinflammatory activity of all patients was A1 or greater, and 33 patients (83%) had a fibrosis score of F1 or greater. Among patients receiving tacrolimus for immunosuppression, the median serum trough level was 5.95 ng/mL (range, 3.3–10.9).

Effect of maintenance interferon therapy on liver histology

To evaluate the efficacy of long-term peginterferon therapy on histological changes, we compared scores between final biopsy samples (median, 44.0 months; range, 24.0–81.3 months) and those taken prior to treatment. Five patients in the non-SVR-IFN group discontinued maintenance

therapy between 26.5 and 53.1 months after the initiation of the treatment because of the adverse events. For these patients, the biopsies taken just before or within 3 months after discontinuation of the treatment were analysed as final biopsies. Despite the variation in time between pretreatment and final biopsy sample collection, there were no significant differences in the duration among the three groups ($P = 0.547$). Median duration from initiation of interferon therapy to final liver biopsy was 41.9 months (range, 24.0–81.3 months) in the SVR group, 41.7 months (range, 26.5–68.4 months) in the non-SVR-IFN group and 46.5 months (range, 30.4–79.6 months) in the non-SVR-Withdrawal group.

There were no significant differences in baseline activity grades or fibrosis stages of patients in the three treatment groups when they were first diagnosed with recurrent hepatitis C (Table 1). However, there were noticeable differences among the three groups by the end of treatment (Fig. 2a). The activity grade of all patients in the SVR and non-SVR-IFN groups improved or remained stable, whereas it deteriorated in 6 (50%) of 12 patients in the non-SVR-Withdrawal group. The fibrosis stage deteriorated in all patients in the non-SVR-Withdrawal group; nine of these patients (75%) deteriorated by more than one stage. In contrast, only four patients (24%) in the non-SVR-IFN group deteriorated, all by only a single stage. Furthermore, three patients actually improved. In the SVR group, fibrosis stage decreased or remained stable in 10 of 11 patients (91%).

In patients in the SVR and non-SVR-IFN groups, the mean activity grade was markedly reduced in the final biopsy, compared to the pretreatment biopsy (Fig. 2b). In contrast, patients in the non-SVR-Withdrawal group experienced an increase in activity grade. The differences between the non-SVR-Withdrawal group and both the SVR and the non-SVR-IFN groups were statistically significant ($P < 0.001$). The mean changes in fibrosis stage in the SVR and non-SVR-IFN groups were −0.18 and +0.06, respectively, suggesting that fibrosis did not change during the follow-up period. However, there was an obvious increase (+2.2) among patients in the non-SVR-Withdrawal group, indicating marked progression of fibrosis.

The Kaplan–Meier analysis allowed us to investigate whether patients in the three treatment groups experienced different progression rates to late-stage fibrosis (Fig. 2c). No patient in the SVR group and only 1 patient (6%) in the non-SVR-IFN group developed fibrosis stage F3 or F4, whereas nine patients (75%) in the non-SVR-Withdrawal group progressed to these stages. The rates of fibrosis progression were significantly higher in the non-SVR-Withdrawal group than in the non-SVR-IFN and SVR groups ($P = 0.0049$ and $P = 0.0086$, respectively). There was no significant difference between the SVR group and the non-SVR-IFN group ($P = 0.3980$). Five-year progression rates to F3 or F4 were 0% in the SVR group, 14% in the non-SVR-IFN group and 54% in the non-SVR-Withdrawal group.

Safety and tolerability of maintenance interferon therapy

Five of 17 patients (29%) who received low-dose maintenance peginterferon treatment discontinued interferon therapy because of biliary complications ($n = 2$), neutropenia ($n = 1$), anaemia ($n = 1$) and *de novo* AIH ($n = 1$), between 26.5 and 53.1 months after its initiation. The biliary complications were not related to interferon therapy. Patients with neutropenia and anaemia recovered after discontinuing interferon therapy and were able to resume therapy within months (3 and 10, respectively). Steroid therapy alleviated the *de novo* AIH, but the patients did not resume interferon therapy.

DISCUSSION

Studies have repeatedly shown the benefits of achieving SVR via interferon therapy after liver transplantation. For instance, the durability of the SVR is associated with improvements in hepatic inflammation and histological regression of fibrosis over the long-term [18–23]. In contrast, efficacy of interferon therapy for non-SVR patients after liver transplantation had not previously been investigated. Here, we have demonstrated that long-term peginterferon maintenance therapy suppresses histological progression of recurrent hepatitis C after LDLT.

Maintenance interferon therapy was recently shown to have no influence on either histological or clinical outcomes in patients with nontransplant hepatitis C [24]. This conclusion was drawn after observing that the rate of fibrosis progression was similar between treatment and control groups following a 3.5-year randomized controlled trial of low-dose peginterferon. As a large number of patients with advanced fibrosis were enrolled in the randomized controlled trial, it is difficult to compare with our study in which the number of patients studied is much smaller and patients with advanced fibrosis were not enrolled. In the current study after liver transplantation, however, we demonstrated that low-dose maintenance interferon therapy reduced necroinflammatory activity and fibrosis scores in non-SVR patients to levels similar to those in SVR patients. Furthermore, we found that non-SVR patients who discontinued treatment had significantly worse scores once no longer receiving therapy.

Although these results clearly suggest that low-dose peginterferon maintenance therapy is beneficial for non-SVR patients with recurrent hepatitis C after liver transplantation, the mechanism behind this positive response is unknown. Progression of hepatitis C and development of fibrosis after discontinuation of interferon treatment has been shown to proceed more rapidly in patients who have undergone liver transplantation [20,21]. Our results, indicating that activity grade and fibrosis stage markedly deteriorated in non-SVR patients who discontinued maintenance treatment, support these previous findings. Thus, such a

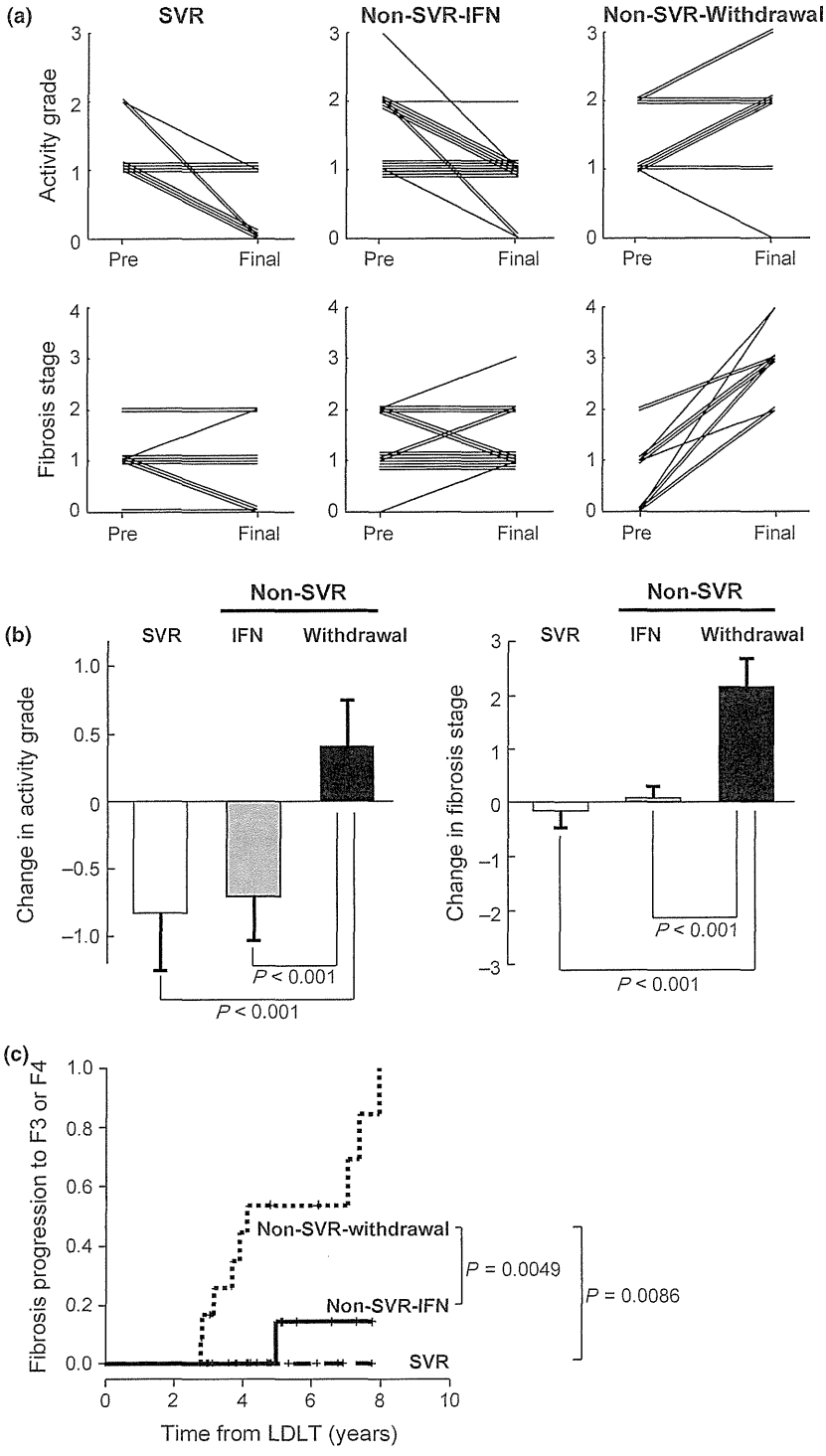

Fig. 2 Effect of maintenance interferon therapy on liver histology: (a) Changes in activity grade (upper) and fibrosis score (lower) of individual patients before interferon therapy (Pre) and at final biopsy (final). (b) Mean changes of liver activity grade (left) and fibrosis stage (right) between pretreatment liver biopsy and the final liver biopsy in each of the three treatment groups. The error bars represent 2 SEs. (c) Kaplan–Meier estimates of the progression rates among patients whose fibrosis advanced to F3 or F4. The dashed line indicates the sustained virological response (SVR) group, the solid line indicates the non-SVR-IFN group and the dotted line indicates the non-SVR-Withdrawal group.

rapid progression of recurrent hepatitis C in patients who discontinued interferon therapy may have highlighted the beneficial effect of the low-dose peginterferon maintenance therapy.

Another issue is the tolerability and safety of long-term peginterferon maintenance treatment. In this study, five patients (29%) discontinued the treatment during the peginterferon maintenance treatment, but only three did so for reasons directly related to the treatment. While two of these patients recovered simply by discontinuing the treatment, the third did require steroid pulse therapy to treat *de novo* AIH. Overall, however, the maintenance therapy did not result in the incidence of major adverse events, suggesting that it is both a tolerable and a safe treatment method.

Our work shows that long-term, low-dose peginterferon administration is an effective method for inhibiting the

progression of liver damage for recurrent hepatitis C after liver transplantation. Unfortunately, this was not a randomized control study, and only a small number of patients were eligible for research. Therefore, we recommend further work to more fully explore the effects of this treatment and to improve the outcomes for patients who do not achieve SVR.

ACKNOWLEDGEMENTS

This work was supported by Grants-in-aid for Scientific Research from the Ministry of Education, Culture, Sports, Science and Technology of Japan; and the Ministry of Health, Labour and Welfare of Japan.

REFERENCES

1 Berenguer M, Prieto M, San Juan F *et al.* Contribution of donor age to the recent decrease in patient survival among HCV-infected liver transplant recipients. *Hepatology* 2002; 36(1): 202–210.
2 Feray C, Caccamo L, Alexander GJ *et al.* European collaborative study on factors influencing outcome after liver transplantation for hepatitis C. European Concerted Action on Viral Hepatitis (EUROHEP) Group. *Gastroenterology* 1999; 117(3): 619–625.
3 Forman LM, Lewis JD, Berlin JA, Feldman HI, Lucey MR. The association between hepatitis C infection and survival after orthotopic liver transplantation. *Gastroenterology* 2002; 122(4): 889–896.
4 Gane E. The natural history and outcome of liver transplantation in hepatitis C virus-infected recipients. *Liver Transpl* 2003; 9(11): S28–S34.
5 Prieto M, Berenguer M, Rayon JM *et al.* High incidence of allograft cirrhosis in hepatitis C virus genotype 1b infection following transplantation: relationship with rejection episodes. *Hepatology* 1999; 29(1): 250–256.
6 Sanchez-Fueyo A, Restrepo JC, Quinto L *et al.* Impact of the recurrence of hepatitis C virus infection after liver transplantation on the long-term viability of the graft. *Transplantation* 2002; 73(1): 56–63.
7 Velidedeoglu E, Mange KC, Frank A *et al.* Factors differentially correlated with the outcome of liver transplantation in hcv+ and HCV- recipients. *Transplantation* 2004; 77(12): 1834–1842.
8 Gordon FD, Kwo P, Vargas HE. Treatment of hepatitis C in liver transplant recipients. *Liver Transpl* 2009; 15(2): 126–135.
9 Terrault NA. Hepatitis C therapy before and after liver transplantation. *Liver Transpl* 2008; 14(Suppl. 2): S58–S66.
10 Berenguer M. Systematic review of the treatment of established recurrent hepatitis C with pegylated interferon in combination with ribavirin. *J Hepatol* 2008; 49(2): 274–287.
11 Kuo A, Terrault NA. Antiviral therapy in liver transplant recipients: is SVR the only endpoint that matters? *J Hepatol* 2007; 46(3): 359–361.
12 Ueda Y, Takada Y, Haga H *et al.* Limited benefit of biochemical response to combination therapy for patients with recurrent hepatitis C after living-donor liver transplantation. *Transplantation* 2008; 85(6): 855–862.
13 Ueda Y, Takada Y, Marusawa H, Egawa H, Uemoto S, Chiba T. Individualized extension of pegylated interferon plus ribavirin therapy for recurrent Hepatitis C genotype 1b after living-donor liver transplantation. *Transplantation* 2010; 90(6): 661–665.
14 Bedossa P, Poynard T. An algorithm for the grading of activity in chronic hepatitis C. The METAVIR Cooperative Study Group. *Hepatology* 1996; 24(2): 289–293.
15 Poynard T, Bedossa P, Opolon P. Natural history of liver fibrosis progression in patients with chronic hepatitis C. The OBSVIRC, METAVIR, CLINIVIR, and DOSVIRC groups. *Lancet* 1997; 349(9055): 825–832.
16 Ueda Y, Takada Y, Marusawa H *et al.* Clinical features of biochemical cholestasis in patients with recurrent hepatitis C after living-donor liver transplantation. *J Viral Hepat* 2010; 17(7): 481–487.
17 Ohno O, Mizokami M, Wu RR *et al.* New hepatitis C virus (HCV) genotyping system that allows for identification of HCV genotypes 1a, 1b, 2a, 2b, 3a, 3b, 4, 5a, and 6a. *J Clin Microbiol* 1997; 35(1): 201–207.
18 Abdelmalek MF, Firpi RJ, Soldevila-Pico C *et al.* Sustained viral response to interferon and ribavirin in liver transplant recipients with recurrent hepatitis C. *Liver Transpl* 2004; 10(2): 199–207.
19 Bizollon T, Ahmed SN, Radenne S *et al.* Long term histological improvement and clearance of intrahepatic hepatitis C virus RNA following sustained response to interferon-ribavirin combination therapy in liver transplanted patients with hepatitis C virus recurrence. *Gut* 2003; 52(2): 283–287.
20 Bizollon T, Pradat P, Mabrut JY *et al.* Benefit of sustained virological response to combination therapy on graft survival of liver transplanted patients with recurrent chronic hepatitis C. *Am J Transplant* 2005; 5(8): 1909–1913.
21 Carrion JA, Navasa M, Garcia-Retortillo M *et al.* Efficacy of antiviral therapy on hepatitis C recurrence after liver transplantation: a randomized controlled study. *Gastroenterology* 2007; 132(5): 1746–1756.
22 Fernandez I, Meneu JC, Colina F *et al.* Clinical and histological efficacy of pegylated interferon and ribavirin therapy of recurrent hepatitis C after liver transplantation. *Liver Transpl* 2006; 12(12): 1805–1812.
23 Toniutto P, Fabris C, Fumo E *et al.* Pegylated versus standard interferon-alpha in antiviral regimens for post-transplant recurrent hepatitis C: comparison of tolerability and efficacy. *J Gastroenterol Hepatol* 2005; 20(4): 577–582.
24 Di Bisceglie AM, Shiffman ML, Everson GT *et al.* Prolonged therapy of advanced chronic hepatitis C with low-dose peginterferon. *N Engl J Med* 2008; 359(23): 2429–2441.

exhibit linear clearance, suggesting that larger individuals clear antibodies more rapidly than smaller individuals without compensatory increases in FcRn-mediated salvage. The effects of other demographic factors, such as age, gender, and renal or hepatic function on the pharmacokinetics of antibodies, are controversial and rarely reported.

An additional clearance mechanism is the development of an immune response against the therapeutic antibody (eg, anti-infliximab or anti-adalimumab antibodies). This affects the pharmacokinetics by increasing clearance, and/or impairing binding. Antiglobulin responses are classed as neutralizing or non-neutralizing, depending on their effect on the activity of the antibody. All therapeutic antibodies approved to date have shown some immunogenicity, even in immunosuppressed patients, although relatively short halve-lives for some chimeric antibodies relative to their FcRn-binding affinity may be related to an enhanced immunogenic response in comparison with human antibodies. On the other hand, the route of administration can sometimes affect immunogenicity, with the intravenous route of administration usually being the least immunogenic. Generally, the intramuscular and subcutaneous routes are more immunogenic. Testing immunogenicity of infliximab and adalimumab in the particular disease of interest is paramount also to understand differential therapeutic effects.

Finally, concomitant administration of other agents that may affect antibody clearance by competing for binding sites, reducing receptor density, or affecting immunogenicity must be considered as potentially affecting clearance. In particular, the role of cotreatment with corticosteroids or immunosuppressive drugs should be further clarified. Beside their impact on therapeutic antibodies immunogenicity, an effect on non–immune-mediated clearance has also been suggested.

Although based on available evidence, the magnitude and the relevance of the correlation between trough levels of anti-TNF therapeutic antibodies and clinical response in inflammatory bowel disease remains unclear, particularly for adalimumab, nonresponders or patients losing response very often have low trough levels. All these considerations point to the urgent need to perform a fine and precise pharmacokinetic profiling, and characterize the pharmacokinetics–pharmacodynamics relationship very early in the development of an antibody therapy, and for any new therapeutic indication. This is key for more successful drug development and to provide greater benefit to patients.

EDOUARD LOUIS
University Hospital CHU of Liège
Liège, Belgium

JULIÁN PANÉS
Hospital Clínic Barcelona
IDIBAPS, CIBERehd
Barcelona, Spain

LARGE-SCALE IDENTIFICATION OF EFFECTOR GENES THAT MEDIATE THE TYPE I INTERFERON ANTIVIRAL RESPONSE

Schoggins JW, Wilson SJ, Panis M, et al. A diverse range of gene products are effectors of the type I interferon antiviral response. Nature 2011;472:481–485.

Type I interferons (IFNs) are multifaceted cytokines with a central role in the host innate defense against viral infection. Upon viral infection, the host elicits a type I IFN response, mediated essentially by the expression of hundreds of IFN-stimulated genes (ISGs; Annu Rev Immunol 2005;23:307–336). Although it is assumed that these ISGs function together and are required for establishment of the antiviral state, few have been characterized regarding their antiviral potential, target specificity, and mechanisms of action.

To address these issues, in their recently published paper in the *Nature*, researchers at the Rockefeller University in New York conducted a large-scale, fluorescence-activated, cell sorting-based screen of antiviral ISGs. Based on previously published microarray gene expression data, the authors selected 389 human ISGs as candidate effector genes for screening. Each selected ISG was inserted into a bicistronic lentiviral vector co-expressing the red fluorescent protein TagRFP. The generated lentiviral ISG stocks were used for the transduction of target cells. ISG-TagRFP–expressing target cells were then challenged with a panel of green fluorescent protein-expressing viruses, and viral replication was monitored by quantification of the green fluorescent protein-positive cells in the RFP-positive population. This high-throughput screening strategy allowed for sensitive, quantitative, and systematic evaluation of the antiviral effect of individual ISGs against several medically important viruses, including hepatitis C virus (HCV), HIV, yellow fever virus, West Nile virus, Venezuelan equine encephalitis virus, and chikungunya virus.

Through extensive screening and subsequent validation experiments, they demonstrated that each virus tested was susceptible to inhibition by a unique set of ISGs, with the overall ISG inhibition profile overlapping among viruses. Antiviral ISG hits included broad-acting effectors and specific effectors: The former ISGs including *IRF1, RIG-I, MDA5,* and *IFITM3* showed broad effects on multiple viruses, whereas the latter ISGs, including *DDX60, IFI44L, IFI6,* and *MOV10,* had specific effects on limited viral species. Based on the magnitude of their antiviral effect, the ISGs were categorized as strong inhibitors that broadly act on IFN-mediated or other signaling pathways and modest inhibitors that may have more specific effector functions. Gene ontology analysis classified these validated ISG hits into 3 main molecular functions—nucleic acid binding, hydrolase activity, and helicase activity—and 3 main biologic processes—signal transduction, transcrip-

tion initiation, and small molecule transport. A long-standing hypothesis is that the cooperative action of ISGs is prerequisite for an effective type I IFN response (J Leukoc Biol 2001;69:912–920; Virology 1999;258:435–440). In support of this hypothesis, the authors demonstrated that combinational expression of ISGs generally enhanced their antiviral effects. Surprisingly, they also showed that the expression of several ISGs, including *ADAR, FAM46C, LY6E,* and *MCOLN2,* enhanced viral replication, although how these ISGs do so and why they are induced by IFN signaling remain to be elucidated. Finally, to dissect the antiviral mechanisms of ISGs, they examined the stage of the viral life cycle at which the validated ISGs exert their antiviral functions. The assays using HCV pseudoparticles and subgenomic replicons expressing reporter gene revealed that translational block is the primary and common antiviral mechanism of these effector ISGs, highlighting the surprising host strategy that multiple effectors with diverse molecular functions cooperatively suppress HCV by targeting a single HCV life-cycle stage.

Together, the identification and characterization of novel antiviral effectors presented in this study unraveled the heretofore unsuspected diversity of ISG-mediated IFN effector mechanisms.

Comments. The innate immune response represents the first line of defense against viral assault. Type I IFNs, a family of cytokines with pleiotropic functions, are central players in antiviral innate immunity (Annu Rev Immunol 2005;23:307–336). Since the first description of IFN as a soluble factor produced by influenza virus-infected chick embryo cells that confers resistance to subsequent virus infection (Proc R Soc Lond B 1957;147:258–267), several outstanding studies have contributed to our understanding of many important aspects of IFN system (Immunity 2006;25:343–348). Notably, there is now substantial knowledge about the virus-sensing machineries that lead to type I IFN induction and IFN receptors and their downstream pathway, the so-called JAK–Stat signaling pathway (Nat Immunol 2006;7:131–137; Immunity 2006; 25:361–372).

Activation of the JAK–Stat pathway through IFN receptors induces the expression of numerous ISGs. Most of the well-characterized examples of ISGs are 2′-5′ oligoadenylate synthases, double-stranded RNA-dependent protein kinase R (PKR), and myxovirus resistance proteins. The 2′-5′ oligoadenylate synthases, activated by viral dsRNA, produce 2′-5′ oligoadenylates, which in turn activate the latent nuclease RNase L, resulting in the degradation of viral RNA transcripts as well as host RNAs (Annu Rev Biochem 1998;67:227–264). PKR, a member of the eukaryotic initiation factor 2α kinase family, is another ISG. Activation of PKR by dsRNA results in eukaryotic initiation factor 2α phosphorylation, leading to the translational block of viral and cellular mRNA (Cell 1990; 62:379–390). Myxovirus resistance proteins, large IFN-inducible GTPases of the dynamin family, have antiviral activity against influenza and vesicular stomatitis virus (Cell 1990;62:51–61; Ciba Found Symp 1993;176:233–243). Their similarity with dynamin suggests that they interfere with viral assembly and trafficking in the cell. Furthermore, in association with HCV, ISG56 was recently demonstrated to suppress HCV RNA translation through direct interaction with eIF3, which blocks ribosome recruitment to the viral RNA (J Virol 2004;78: 11591–11604).

Although these examples clearly suggest that ISGs represent essential effector components of IFN signaling to establish an "antiviral state" and indeed hundreds of ISGs have been identified since their discovery >25 years ago (Proc Natl Acad Sci U S A 1979;76:1824–1828; Proc Natl Acad Sci U S A 1984;81:6733–6737; J Leukoc Biol 2001; 69:912–920), the majority of ISGs remain to be characterized with respect to their antiviral activity. Thus, "antiviral state" is a generic term and the larger picture of how the IFN system exerts an antiviral response through the induction of numerous ISGs has long been an open question for most researchers in this field.

These novel findings presented by Schoggins et al provide a long-sought answer for this challenging theme. Overcoming the technical barriers that hampered the systematic overexpression of hundreds of genes, they developed an elegant, cell-based screening system by which they identified multiple novel antiviral ISGs. The major findings of this study are as follows. Each ISG has a diverse range of antiviral potential and virus target specificity. ISGs exert their antiviral effect in a combinatorial fashion, and translational inhibition is a common mechanism of ISG-mediated antiviral action. These findings, together with the fact that IFN therapy is currently the first-choice therapy for HCV eradication and is also used for the treatment of several other viral infections, have potentially important implications for the development of new antiviral therapies. The side effects of IFN therapy, which frequently limit its clinical use, may be due to undesirable global ISG expression. Thus, selective utilization of ISG sets optimized for target viruses might be a more effective and safer therapeutic option.

This work is very exciting and expands our knowledge of downstream IFN effector mechanisms. However, some issues remain to be resolved in future studies. First, the effects of viral evasion mechanisms are dismissed in this study. Most viruses have evolved unique strategies to interfere with various aspects of the IFN system (Nat Rev Immunol 2002;2:675–687). For example, HCV is equipped with multiple evasion mechanisms: NS3/4A serine protease blockade of type I IFN production by the cleavage of IPS-1, a key signaling molecule of the IFN-inducing pathway (Trends Immunol 2006;27:1–4), disruption of JAK–Stat signaling by NS5A, and inhibition of PKR by NS5A and E2 proteins (Nat Rev Immunol 2002;2:675–687). The overexpression platform used in this study may not reflect the events that actually happen during viral infection in vivo. Second, further investigation of the proviral ISGs presented in this study is needed. It is of great interest that several ISGs exhibit proviral activity and the data suggest

that the effect of IFN is more complex than previously thought. What are the physiologic functions of proviral ISGs and why does the IFN system induce them? A loss-of-function study might be useful to answer these questions. Finally, the screening assays were performed on only positive-sense RNA viruses (HCV, yellow fever virus, Venezuelan equine encephalitis virus, West Nile virus, and chikungunya virus) and 1 retrovirus (HIV-1), but not on DNA viruses. Yet the host also obviously activates the type I IFN system against DNA viruses, such as cytomegalovirus and herpes simplex virus, utilizing Toll-like receptor 9 and a not-yet identified cytoplasmic DNA sensor molecule(s) (Nat Immunol 2006;7:131–137; Curr Opin Immunol 2010;22:41–47; Biochem Pharmacol 2010;80:1955–1972). Given that DNA viruses have their own viral life cycle and evasion strategies distinct from those of viruses tested here, there might be other antiviral ISG profiles with mechanisms of action that are entirely unique to DNA viruses. Elucidation of these issues, together with further dissection of the antiviral mechanisms of the validated ISGs, would provide additional insight into the type I IFN antiviral response.

In conclusion, this is the first report of a comprehensive evaluation of antiviral potentials of ISGs. A newly developed, cell-based screening assay identified multiple novel antiviral effectors in the type I IFN system that were previously unanalyzable. Given that current IFN therapy has undesirable side effects, this work opens the door to designing new therapeutic strategies based on antiviral ISGs.

KEN TAKAHASHI
HIROYUKI MARUSAWA
TSUTOMU CHIBA
Department of Gastroenterology and Hepatology
Graduate School of Medicine, Kyoto University
Kyoto, Japan

DIAGNOSTIC ENDOSCOPIC RETROGRADE PANCREATOGRAPHY FOR AUTOIMMUNE PANCREATITIS: ONE SIZE DOES NOT FIT ALL

Sugumar A, Levy MJ, Kamisawa T, et al. Endoscopic retrograde pancreatography criteria to diagnose autoimmune pancreatitis: an international multicentre study. Gut 2011;60:666–670.

Autoimmune pancreatitis (AIP) is being increasingly recognized worldwide. Although the exact etiology and pathogenesis of AIP remain unclear, we do have some insights into the disease process. It has been proposed that AIP is the pancreatic manifestation of an immunoglobulin (Ig)G4-associated systemic fibro-inflammatory disorder that can also affect the bile duct, kidneys, retroperitoneum, orbits, lymph nodes, and salivary glands (Pancreatology 2006;6:132–137). Histologically, AIP is characterized by an inflammatory process, with infiltration of the pancreas by a lymphoplasmactic infiltrate rich in IgG4-positive cells. The inflammatory process can be focal or diffuse. Additionally, IgG4-positive plasma cells and other inflammatory cells have been described as infiltrating other organs in patients with AIP (J Gastroenterol 2003;38:982–984), thus supporting the notion that this process may be systemic. Clinically, AIP presents most commonly as obstructive jaundice; this presentation can often be confused with pancreatic adenocarcinoma. Less commonly, AIP can present with abdominal pain or acute pancreatitis. AIP is treated with a course of corticosteroids, and the response to treatment is often dramatic. A reliable and accurate diagnosis of the disease, particularly differentiation from pancreatic adenocarcinoma, which AIP can mimic, continues to present a clinical challenge (Clin Gastroenterol Hepatol 2006;4:1010–1016; Am J Gastroenterol 2003;98:2694–2699). Histology, considered to be the gold standard for diagnosis, requires a biopsy that is often not easily obtainable in the pancreas. Fine-needle aspiration of the pancreas, although readily available, does not yield a definitive diagnosis of AIP (Clin Gastroenterol Hepatol 2006;4:1010–1016). A core biopsy may be diagnostic, with the caveat that, with patchy distribution of disease or in the presence of a strong desmoplastic reaction, even a core specimen may not yield a diagnosis. Thus, in the appropriate clinical setting, a negative biopsy does not exclude pancreatic cancer or AIP. A surgical biopsy, although certainly not feasible in all cases, may thus be required for diagnosis. Investigators in Asia and the United States have developed several diagnostic classification systems based on clinical, imaging, laboratory, and pathologic criteria, and response to treatment. According to the Japanese Pancreas Society, a diagnosis of AIP can be made when a patient exhibits $\geq$1 imaging feature and either 1 serologic or histologic feature. The Mayo HISORt criteria are more commonly used in the United States, and include $\geq$1 of the following: diagnostic histology, characteristic imaging, elevated serum IgG4 levels, involvement of other organ systems, and response to treatment with glucocorticoids. Although there seems to be an emerging consensus toward uniformity in the criteria, some major differences remain, 1 of which is the use of endoscopic retrograde cholangiopancreatography (ERCP)for ductal imaging; the Asian criteria mandate endoscopic retrograde pancreatography (ERP) for ductal imaging (J Gastroenterol 2006;41:626–631), whereas the Mayo HISORt criteria do not (J Gastroenterol 2007;42[Suppl 18]:39–41).

To advance our understanding of AIP, an international group of experts has formed the Autoimmune Pancreatitis International Cooperative Study group. Given the discrepancy in the use of ERP to diagnose AIP, 1 of the first goals of this collaboration was to determine the performance characteristics of ERP for the diagnosis of AIP.

Sugumar et al performed an international, multicenter study in 2 phases (Gut 2011;60:666–670). A total of 21 physicians from 4 centers in Asia, the United Kingdom,

uicc
global cancer control

IJC
International Journal of Cancer

Excessive activity of apolipoprotein B mRNA editing enzyme catalytic polypeptide 2 (APOBEC2) contributes to liver and lung tumorigenesis

Shunsuke Okuyama, Hiroyuki Marusawa, Tomonori Matsumoto, Yoshihide Ueda, Yuko Matsumoto, Yoko Endo, Atsushi Takai and Tsutomu Chiba

Department of Gastroenterology and Hepatology, Graduate School of Medicine, Kyoto University, Shogoin, Sakyo-Ku, Kyoto, Japan

Apolipoprotein B mRNA editing enzyme catalytic polypeptide 2 (APOBEC2) was originally identified as a member of the cytidine deaminase family with putative nucleotide editing activity. To clarify the physiologic and pathologic roles, and the target nucleotide of APOBEC2, we established an APOBEC2 transgenic mouse model and investigated whether APOBEC2 expression causes nucleotide alterations in host DNA or RNA sequences. Sequence analyses revealed that constitutive expression of APOBEC2 in the liver resulted in significantly high frequencies of nucleotide alterations in the transcripts of eukaryotic translation initiation factor 4 gamma 2 (*Eif4g2*) and phosphatase and tensin homolog (*PTEN*) genes. Hepatocellular carcinoma developed in 2 of 20 APOBEC2 transgenic mice at 72 weeks of age. In addition, constitutive APOBEC2 expression caused lung tumors in 7 of 20 transgenic mice analyzed. Together with the fact that the proinflammatory cytokine tumor necrosis factor-α induces ectopic expression of APOBEC2 in hepatocytes, our findings indicate that aberrant APOBEC2 expression causes nucleotide alterations in the transcripts of the specific target gene and could be involved in the development of human hepatocellular carcinoma through hepatic inflammation.

The number of coding sequences in the genome is limited, but the genomic information encoded in DNA or RNA sequences can be manipulated to produce a wide range of expression products in cells.[1] Apolipoprotein B mRNA editing enzyme catalytic polypeptide (APOBEC) family members are nucleotide-editing enzymes capable of inserting somatic mutations in DNA and/or RNA through their cytidine deaminating activity.[2] The APOBEC family comprises APOBEC1, -2, -3A, -3B, -3C, -3DE, -3F, -3G, -3H, -4, activation-induced cytidine deaminase (AID) in humans, and APOBEC1, -2, -3, and AID in mice, and contribute to producing various physiologic outcomes by modifying target gene sequences.[3–5] For example, APOBEC1 participates in lipid metabolism by deaminating a specific cytidine to uridine in Apolipoprotein (Apo-) B transcript sequences. The nucleotide change induced by APOBEC1 activity results in the formation of a termination codon in an Apo-B48 mRNA, leading to the production of molecules about half the size of a full-length genomically encoded Apo-B100.[6,7] APOBEC3G is a cytidine deaminase that induces hypermutation in viral DNA sequences and acts as a host defense factor against various viruses, including HIV-1 and hepatitis B viruses.[8–15] On the other hand, AID is expressed in germinal center B-cells and induces somatic hypermutation and class switch recombination of the immunoglobulin genes encoded in human DNA sequences, resulting in the amplification of immune diversity.[16,17] APOBEC1, APOBEC3G and AID thus create nucleotide changes in their preferential target DNA or RNA structures. In contrast to these APOBEC proteins, little is known about the function and editing activity of APOBEC2. Although previous reports indicate that murine APOBEC2 mRNA and protein are expressed exclusively in heart and skeletal muscle, the substrate and function of APOBEC2 and whether APOBEC2 has nucleotide editing activity remain unknown.[18,19]

Accumulating evidence suggests that excessive or aberrant activity of APOBEC family members leads to tumorigenesis through their nucleotide editing of tumor-related genes.

Key words: APOBEC2, hepatocellular carcinoma, lung cancer

Abbreviations: APOBEC: Apolipoprotein B mRNA editing enzyme catalytic polypeptide; EIF4G2: Eukaryotic translation initiation factor 4 gamma 2; AID: activation-induced cytidine deaminase; Apo-: Apolipoprotein; Tg: transgenic; NF-κB: nuclear factor-κB; HCC: hepatocellular carcinoma; TNF: tumor necrosis factor; cDNA: Complimentary DNA; RT-PCR: real-time reverse-transcription polymerase chain reaction; ER: estrogen receptor

Additional Supporting Information may be found in the online version of this article.

Grant sponsors: Japan Society for the Promotion of Science (JSPS), a Grant from the Ministry of Health, Labor, and Welfare, Japan, the Takeda Science Foundation

DOI: 10.1002/ijc.26114

History: Received 8 Jan 2011; Accepted 25 Mar 2011; Online 5 Apr 2011

Correspondence to: Hiroyuki Marusawa, MD, PhD, Department of Gastroenterology and Hepatology, Graduate School of Medicine, Kyoto University, 54 Kawahara-cho, Shogoin, Sakyo-ku, Kyoto 606-8507, Japan, Tel.: +81-75-751-4302, Fax: +81-75-751-4303, E-mail: maru@kuhp.kyoto-u.ac.jp

Transgene expression of APOBEC1 causes dysplasia and carcinoma in mouse and rabbit liver due to its aberrant editing of the eukaryotic translation initiation factor 4 gamma 2 (Eif4g2).[20,21] A more striking tumor phenotype is observed in mice with constitutive and ubiquitous AID expression. We previously demonstrated that AID transgenic (Tg) mice developed tumors in various organs, including liver, lung, stomach and lymphoid organs, accompanied by the accumulation of somatic mutations on several tumor-related genes such as *Tp53* and *Myc*.[22,23] Interestingly, we also found that proinflammatory cytokine stimulation induces a substantial upregulation of APOBEC2 transcription *via* the activation of the transcriptional factor nuclear factor-κB (NF-κB) in hepatoma-derived cells, whereas only trace amounts of endogenous APOBEC2 expression are detectable in normal hepatocytes.[24] On the basis of the fact that most human hepatocellular carcinoma (HCC) arises in the setting of chronic liver disease with the features of chronic hepatitis or liver cirrhosis, we hypothesized that APOBEC2 enzyme activity has a role in the accumulation of genetic alterations in tumor-related genes under conditions of hepatic inflammation, thereby contributing to the development of HCC. In this study, we investigated the putative nucleotide editing ability of APOBEC2 on the host genes in hepatocytes, and its relevance to carcinogenesis by establishing Tg mice that constitutively express APOBEC2.

Material and Methods

APOBEC2 Tg mice

Total RNA was extracted from murine liver using Sepasol-RNA 1 Super (Nacalai Tesque, Kyoto, Japan) according to the manufacturer's protocol. Complimentary DNA (cDNA) was synthesized from total RNA with random hexamer primers using a Transcriptor First Strand cDNA Synthesis Kit (Roche, Mannheim, Germany). After amplification of the murine APOBEC2 gene using high-fidelity Phusion Taq polymerase (Finnzymes, Espoo, Finland) with oligonucleotide primers, 5′-GCAGAATTCCACCATGGCTCAGAAGGAAG AGGC-3′(forward) and 5′-ACTCTCGAGCCTACTTCAGGA TGTCTGCC-3′ (reverse), murine APOBEC2 cDNA (1.2 kbp) was cloned downstream of the chicken β-actin (CAG) promoter. The purified fragment of the CAG promoter and APOBEC2 transgene was microinjected into fertilized eggs of the Slc:BDF1, the hybrid of C57BL/6CrSlc and DBA/2CrSlc (Japan SLC, Shizuoka, Japan), to generate APOBEC2 Tg mice. Tg mice were maintained in specific pathogen-free conditions at the Institute of Laboratory Animals of Kyoto University. Control mice were littermates carrying no transgene. Tissue samples from Tg mice were removed and fixed in 4% (w/v) formaldehyde, embedded in paraffin, stained with hematoxylin and eosin and examined for histologic abnormalities. Tissue samples were also frozen immediately in liquid nitrogen for nucleotide extraction. The mice received humane care according to the "Guide for the Care and Use of Laboratory Animals" prepared by the National Academy of Sciences and published by the National Institutes of Health, USA (NIH publication 86-23).

Quantitative real-time reverse transcription PCR

Quantitative real-time reverse-transcription polymerase chain reaction (RT-PCR) for murine *APOBEC1* and *APOBEC2* amplification was performed using a LightCycler® 480 instrument (Roche). cDNA was synthesized from 1 μg of total RNA isolated from the cells with random hexamer primers in a total volume of 20 μL using Transcriptor First Strand cDNA Synthesis Kit (Roche). Real-time PCRs were set up in 20 μL of FastStart Universal SYBR Green (Roche) with the RT product and the following oligonucleotide primers: APOBEC1, 5′-CGAAGCTTATTGGCCAAGGT-3′ (forward) and 5′-AAGGAGATGGGGTGGTATCC-3′ (reverse); APOBEC2, 5′-CCCTTCGAGATTGTCACTGG-3′ (forward) and 5′-TGTTCATCCTCCAGGTAGCC-3′ (reverse). Target cDNAs were normalized to the endogenous RNA levels of the housekeeping reference gene for *18S ribosomal RNA* (*18S rRNA*).[25] For simplicity, the expression levels of *APOBEC2* are represented as relative values compared with the control specimen in each experiment.

Immunoblotting

Homogenates of murine specimens were diluted in 2× sodium dodecyl sulfate sample buffer (62.5 mM Tris-HCl, pH 6.8; 2% SDS; 5% β-mercaptoethanol; 10% glycerol, and 0.002% bromophenol blue) and boiled for 5 min. Protein samples were separated by sodium dodecyl sulfate-polyacrylamide gel electrophoresis on 12% (w/v) polyacrylamide gels and subjected to immunoblotting analysis.[26] A polyclonal antibody against human and murine APOBEC2 was generated using purified recombinant APOBEC2 protein as an immunogen. A mouse monoclonal antibody against α-tubulin was purchased from Calbiochem (San Diego, CA).

Cell culture and transfection

Human hepatoma-derived cell lines HepG2 and Huh7 were maintained in Dulbecco's modified Eagle's medium (Gibco-BRL) containing 10% fetal bovine serum. Trans-IT 293 transfection reagent (Mirus Bio Corporation, Madison, WI) was used for plasmid transfection. To generate stable cell lines, pcDNA3-ERT2 was made by inserting the ERT2 fragment, which was cut out from pERT2[27] with *Bam*HI and *Eco*RI. pcDNA3-APO2-ERT2 was made by inserting the PCR-amplified coding sequence of human *APOBEC2*, which was synthesized by RT-PCR with the oligonucleotide primers 5′-ATAGG TACCATGGCCCAGAAGGAAGAGGC-3′ (forward) and 5′-ATAGGATCCAGCTTCAGGATGTCTGCCAAC-3′ (reverse), into the *KpnI-BamHI* site of pcDNA3-ERT2. HepG2 cells were transfected with a *Sca*I-linearized pcDNA3-APO2-ERT2 vector encoding the active form of APOBEC2 fused with the hormone-binding domain of the human estrogen receptor (ER), designated APOBEC2-ER, and cultured in medium

containing G418 (Roche) until colonies of stably transfected clones arose.

Subcloning and sequencing of the target genes

The oligonucleotide primers for the amplification of the human *EIF4G2*, *PTEN*, and *TP53*, and murine *Eif4G2*, *Pten*, *Bcl6* and *Tp53*, genes are shown in Supporting Information Table S1. Amplification of the target sequences was performed using high-fidelity Phusion Taq polymerase (Finnzymes, Espoo, Finland), and the products were subcloned into a pcDNA3 vector (Invitrogen, Carlsbad, CA) using pGEM(R) -T Easy Vector System (Promega, Madison, WI) according to the manufacture's instruction. The resulting plasmids were subjected to sequence analysis as described.[28]

Results

Detection of endogenous APOBEC2 protein expression in hepatocytes

We previously reported that transcription of *APOBEC2* is induced by the proinflammatory cytokine tumor necrosis factor (TNF)-α through the activation of NF-κB. To confirm whether endogenous APOBEC2 protein is elevated in response to TNF-α stimulation in human hepatocytes, we generated a rabbit polyclonal antibody against a common amino-acid sequence to human and murine APOBEC2. Using this anti-APOBEC2 antibody, we first confirmed that plasmid-derived exogenous APOBEC2 protein was efficiently detected by immunoblotting analysis (Fig. 1*a*). We then examined whether endogenous APOBEC2 protein was upregulated by TNF-α stimulation in Huh-7 cells. Immunoblotting analysis using the APOBEC2 antibody revealed that endogenous APOBEC2 protein expression was strongly induced after TNF-α stimulation, suggesting that APOBEC2 protein has a role in hepatocyte function under inflammatory conditions (Fig. 1*b*).

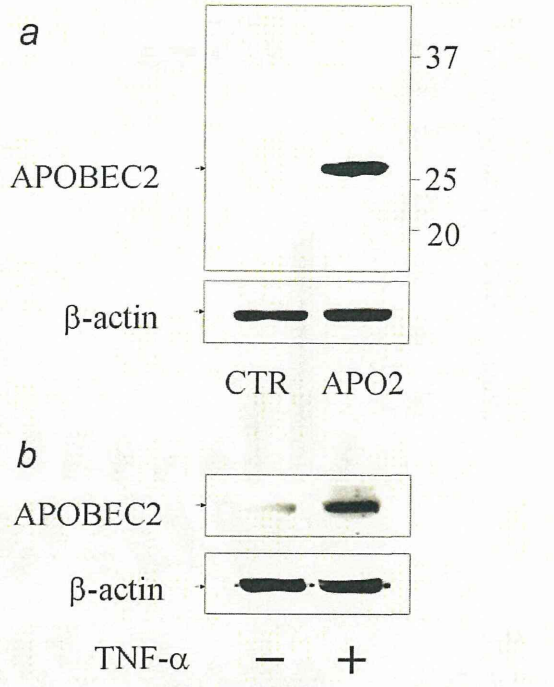

Figure 1. Detection of human APOBEC2 protein in hepatocytes by a specific anti-APOBEC2 antibody. (*a*) Huh7 cells were transfected with plasmid to induce the expression of human APOBEC2 (APO2) or control vector (CTR). After 48 hr, lysates of transfected cells were immunoblotted with anti-APOBEC2 antibody (upper panel) or anti-β-actin antibody (lower panel). (*b*) Huh7 cells were treated with tumor necrosis factor-α (100 ng/ml) for 48 hr followed by immunoblotting using anti-APOBEC2 antibody (upper panel) or anti-β-actin antibody (lower panel).

Establishment of a Tg mouse model constitutively expressing APOBEC2

To investigate the enzymatic activity of APOBEC2 *in vivo*, we generated a Tg mouse model with constitutive and ubiquitous expression of APOBEC2 under the control of CAG promoter. APOBEC2 Tg mice were born healthy and with a body weight similar to that of their wild-type littermates. The expression level of APOBEC2 in various organs of the Tg mice was examined by quantitative RT-PCR and compared with that in the wild-type mice. In wild-type mice, endogenous APOBEC2 transcript was expressed at high levels in heart and skeletal muscle, whereas little or no APOBEC2 expression was detected in the liver, gastrointestinal tracts, lung, spleen and kidney. In contrast, high expression of *APOBEC2* mRNA was ubiquitously detected in the Tg mice, but the expression levels of *APOBEC2* in the liver or lung of the Tg mice were relatively lower than those of the wild-type heart or skeletal muscle (Fig. 2*a*). Immunoblotting analysis using the specific antibodies against APOBEC2 also revealed widespread expression of APOBEC2 protein in various epithelial organs of the Tg mice, with relatively low expression in kidney and spleen (Fig. 2*b*).

Constitutive expression of APOBEC2 resulted in the accumulation of nucleotide alterations in RNA sequences of Eif4g2 and Pten genes in hepatocytes

To clarify whether APOBEC2 targets DNA or RNA, we first extracted total RNA from the nontumor liver tissues of 2 APOBEC2 Tg mice that developed HCC (described below) and their 3 APOBEC2 Tg littermates without any tumor phenotypes, and subjected them to sequence analyses. We chose 2 representative tumor-suppressor genes that are frequently mutated in human cancers, *Pten*, and *Tp53*. The *Bcl6* and *Eif4g2* genes were also included because they are the preferential targets for AID- and APOBEC1-mediated mutagenesis, respectively. We first confirmed that the transcription levels of the genes analyzed for RNA sequencing did not differ between the liver tissues of APOBEC2 Tg mice and wild-type littermates (Supporting Information Fig. S1). In addition, there was no difference in the quantitative levels of APOBEC1 expression between the APOBEC2-expressing liver and

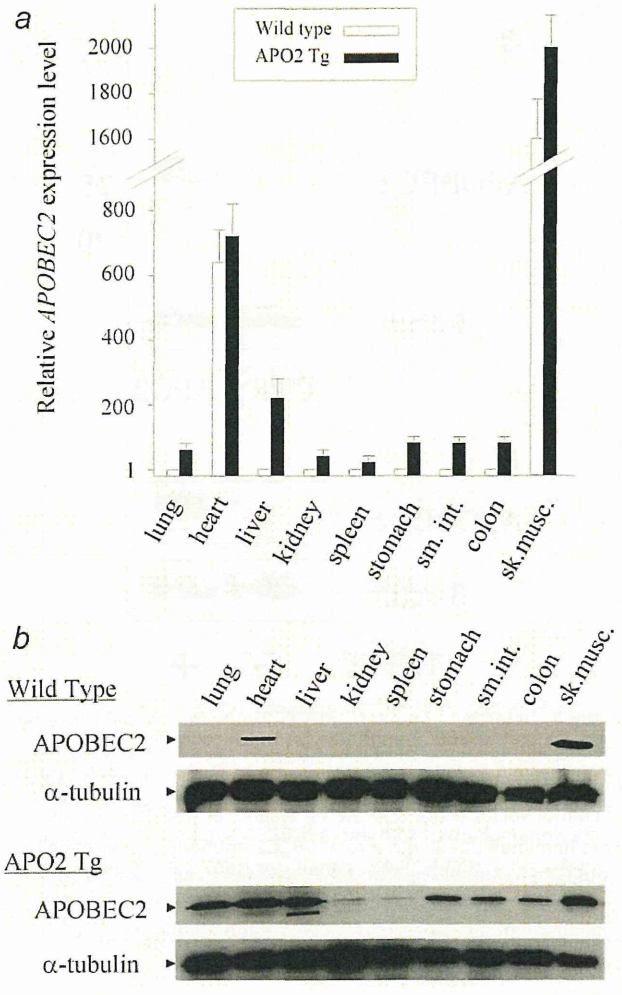

Figure 2. Expression analyses of APOBEC2 Tg mice. (*a*) Relative expression levels of *APOBEC2* transcripts calibrated by the amount of *18S rRNA* for indicated organs of adult APOBEC2 Tg mice (48-week-old) and their wild-type littermates. Data shown are mean results of quantitative real-time RT-PCR analyses for the indicated mouse groups ($n = 6$). Filled bar, APOBEC2 Tg mice; open bar, wild-type mice; sm.int, small intestine; sk.musc, skeletal muscle. (*b*) Results of immunoblot analysis using anti-APOBEC2 (upper panel) or anti-α-tubulin (lower panel) antibody for the lysates of the indicated organs of 48-week-old APOBEC2 Tg mice and their littermates.

normal liver of the wild-type mice (Supporting Information Fig. S2). Sequence analysis revealed a mean of 98,000 and 55,400 base reads per each gene transcript derived from the nontumor liver tissues of the APOBEC2 Tg and control mice, respectively. The total number of amplified clones and RNA sequence reads, and the frequency of nucleotide alterations detected in the nontumor liver tissues of 2 APOBEC2 Tg mice with HCC and the wild-type littermate of the same mouse line are shown in Table 1. The mutation frequencies were highest in the *Eif4g2* transcripts among the genes analyzed in APOBEC2-Tg mice, and were significantly greater compared with those in control tissues (mutation frequencies were 2.75 and 2.36 *vs.* 0.58 substitutions per 1×10^4 nucleotides; $p < 0.05$). Moreover, the nucleotide alteration frequency was significantly higher in the *Pten* gene transcripts from a APOBEC2-expressing liver (Tg-1) than in the control tissues (mutation frequencies were 2.43 *vs.* 0.44 substitutions per 1×10^4 nucleotides, respectively; $p < 0.01$). The *Pten* mRNA of a liver derived from another APOBEC2 Tg mouse (Tg-2; mutation frequency was 1.36 substitutions per 1×10^4 nucleotides) also had a higher nucleotide alteration frequency than that in the control mice, although the difference was not statistically significant ($p = 0.16$ *vs.* control). For the *Eif4g2* and *Pten* transcripts, nucleotide alterations were distributed over the sequences examined and all the alterations detected were different among clones (Fig. 3). Similar results were obtained from the analyses on the liver of 3 APOBEC2 Tg mice that lacked any tumor phenotypes. Indeed, several nucleotide changes had accumulated in both *Eif4g2* and *Pten* transcripts in the liver of all 3 APOBEC2 Tg mice examined (Supporting Information Table S2). In contrast, the mutation frequencies of *Tp53* and *Bcl6* genes of the liver of the APOBEC2 Tg mice were comparable with those of the wild-type mice.

APOBEC2 expression in the liver induced no nucleotide changes in DNA sequences

To clarify whether the nucleotide alterations that emerged in *Eif4g2* and *Pten* transcripts were due to DNA or RNA sequence changes, we determined the DNA sequences of both genes derived from the liver tissues of APOBEC2 Tg and control mice. DNA sequences with an average base length of 0.7 k containing exonic and intronic sequences were amplified, followed by sequence analyses. The total number of amplified clones and DNA sequences read, and the frequency of nucleotide alterations are shown in Supporting Information Table S3. In contrast to the analyses on the RNA sequences, there were no significant differences between the mutation frequency of APOBEC2 Tg mice and that of the wild-type mice of the DNA sequences of the *Eif4g2* and *Pten* genes in the liver. Indeed, no nucleotide alterations were observed in the DNA sequences of the *Eif4g2* gene in the liver of the APOBEC2 Tg mice. Similarly, no mutation was accumulated in the *Pten* DNA sequences of the APOBEC2-expressing liver, suggesting that constitutive expression of the APOBEC2 transgene had no effect on the DNA sequences of the examined regions in the *Eif4g2 and Pten* genes in hepatocytes.

APOBEC2 transgenic mice developed liver and lung tumors

Although most Tg mice were viable at 72 weeks, macroscopic liver and lung tumors developed in some of the APOBEC2 Tg mice. At 72 weeks of age, liver tumors were observed in 2 of 20 Tg male mice, and lung nodules were detected in 7 Tg mice. In contrast to the APOBEC2 Tg mice, none of the wild-type mice developed any tumors at the same age, except 1 with a very small adenoma in the lung. Histopathologic

Table 1. Summary of sequence analysis on the RNA extracted from the liver of the wild-type and APOBEC2 Tg mice

Gene	Mice	Clone	Sequence reads	Nucleotide alterations		
				Number	Frequency(/10^4)	APO2/Wt*
Eif4g2	Wt	82	50,949	3	0.58	
	Tg-1	83	50,835	14	2.75	4.7**
	Tg-2	90	54,986	13	2.36	4.1**
Pten	Wt	92	67,352	3	0.44	
	Tg-1	79	57,599	14	2.43	5.5***
	Tg-2	69	51,323	7	1.36	3.1
Bcl6	Wt	48	41,776	3	0.72	
	Tg-1	59	51,414	1	0.19	0.3
	Tg-2	48	42,413	4	0.94	1.3
Tp53	Wt	84	61,705	2	0.32	
	Tg-1	51	42,285	3	0.71	2.2
	Tg-2	50	40,880	3	0.73	2.3

*Frequency of nucleotide alteration in APOBEC2 Tg mice / in wild type mice. **$p < 0.05$, *vs.* Wt. ***$p < 0.01$, *vs.* Wt.
Abbreviations: Tg, APOBEC2 Tg mice; WT, wild type mice.

analysis of hepatic tumors developed in the APOBEC2 Tg mice revealed nodular aggregates of neoplastic hepatocytes and permeation of tumor cells into residual normal lobules (Fig. 4). Tumor cells had enlarged and hyperchromatic nuclei with chromatin clumping and occasional prominent nucleoli, which were similar to the morphologic characteristics of typical human HCC. On the other hand, lung tumors showed various degrees of cellular atypia, from adenoma to adenocarcinoma (Fig. 5*a*). In addition, monotonous atypical lymphocytes with cytologic features of lymphoblastic lymphoma, such as enlarged round nuclei, irregular nuclear contours, and frequent mitotic figures, massively invaded the spleens of 2 Tg mice (Fig. 5*b*). These findings suggest that constitutive expression of APOBEC2 causes the development of neoplasia in the epithelial organs, including the liver and the lung.

APOBEC2 induced the accumulation of nucleotide alterations of specific target RNA sequences in hepatocytes in vitro

To confirm whether APOBEC2 exerts genotoxic effects on RNA transcripts of the specific target genes, we investigated the alteration frequencies of RNA sequences in cells with constitutive APOBEC2 expression. For this purpose, we established a conditional expression system that allowed for APOBEC2 activation in the cells in response to an estrogen analogue, 4-hydroxytamoxifen (OHT). OHT treatment triggered a posttranslational conformational change and prompt activation of APOBEC2 in APOBEC2-ER expressing cells.[29] We analyzed 3 genes including *PTEN*, *TP53* and *EIF4G2* for the sequence analysis of APOBEC2-mediated mutagenesis *in vitro*. Total RNA was extracted from the APOBEC2-ER expressing HepG2 cells treated with OHT for 8 weeks and the coding RNA sequences of the selected genes were determined by sequence analyses. The total number of amplified clones and RNA sequence reads, and the frequency of nucleotide alterations are shown in Supporting Information Table S4. We found that the emergence of nucleotide alterations in the *PTEN* and *EIF4G2* transcripts was detected at higher frequencies in the cells with APOBEC2 activation compared with control cells treated with OHT, while these differences were not statistically significant ($p = 0.23$ *vs.* control, and $p = 0.39$ *vs.* control, respectively). In contrast, the frequency of nucleotide alterations in the transcripts of the *TP53* in the cells with APOBEC2 activation was comparable with that in the control cells. Similar to the findings obtained from the APOBEC2 Tg mice liver tissues, there were no significant differences between APOBEC2-expressing hepatocytes and control cells in the incidence of nucleotide alterations in the *PTEN* and *EIF4G2* genes (Supporting Information Table S5). These data further suggest that APOBEC2 exerts mutagenic activity in hepatocytes and preferentially achieves nucleotide substitutions in the coding sequences of the specific target genes.

Discussion

Among the APOBEC family members, APOBEC2 and AID homologs can be traced back to bony fish, whereas APOBEC1 and APOBEC3s are restricted to mammals.[30,31] The broad preservation of the APOBEC2 homolog among vertebrates suggests that APOBEC2 has a critical role in the physiology of many species. Little is currently known, however, about the biologic activity of APOBEC2 in any type of cells. Moreover, it is not known whether APOBEC2 possesses nucleotide editing activities like other APOBEC family member proteins. In the present study, we demonstrated for the first time that APOBEC2 expression triggered nucleotide alterations in RNA sequences of the specific genes in hepatocytes. In addition, our findings suggest that APOBEC2 could

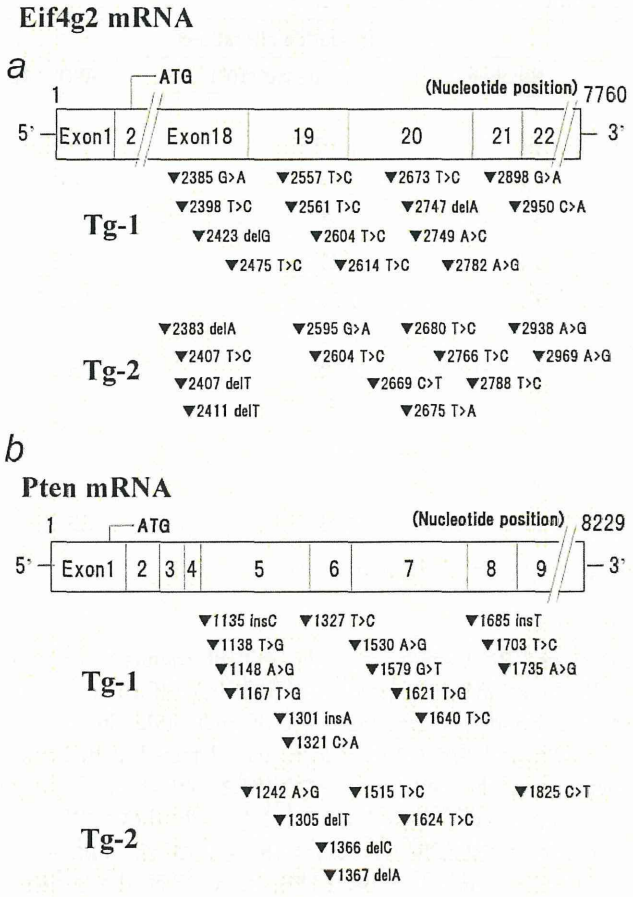

Figure 3. Distribution of nucleotide alterations in the Eif4g2 and Pten trascripts in the APOBEC2-expressing hepatocytes. The mRNA sequences between exon 18 and exon 21 of the Eif4g2 gene (*a*), and the mRNA sequences between exon 5 and exon 8 of the Pten gene (*b*) were determined in the nontumor liver tissues of 2 APOBEC2 Tg mice. The nucleotide positions of the mutations emerged in the Eif4g2 and Pten mRNA of APOBEC2-expressing liver are shown.

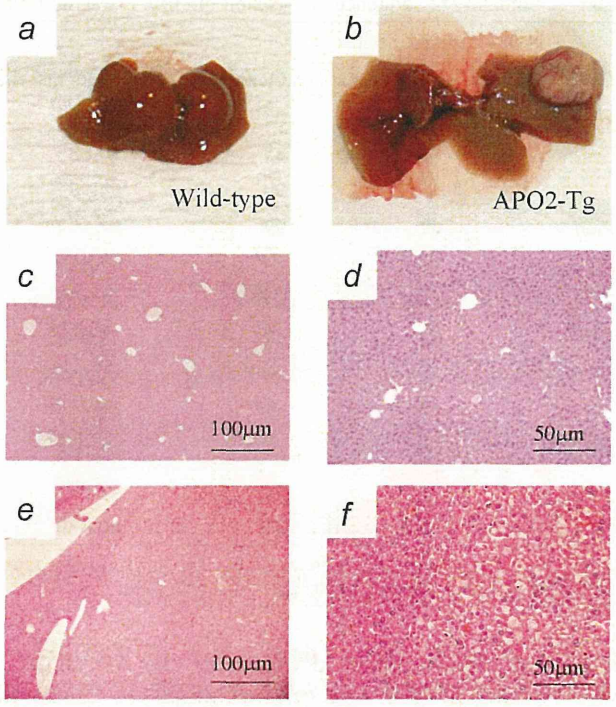

Figure 4. Tumors developed in the liver of APOBEC2 Tg mice. Macroscopic (*b*) and microscopic (haematoxylin and eosin) images (*e, f*) of the HCC that developed in a 72-week-old APOBEC2 Tg mouse and the non-cancerous liver of the same animal (*c,d*). Macroscopic image of the liver of a wild-type littermate is also shown (*a*). (Original magnifications: 3*c,e* ×40; 3*d,f* ×100).

contribute to tumorigenesis via the nucleotide alterations of RNA sequences of the target genes.

On the basis of the close sequence homology of APOBEC2 with other APOBEC proteins, APOBEC2 is thought to exhibit deamination activity to achieve nucleotide editing. Indeed, crystal structure analysis indicates that APOBEC2 contains amino acid residues with 4 monomers in each asymmetric unit that form a tetramer with an atypical elongated shape, and this prominent feature of the APOBEC2 tetramer suggests that the active sites are accessible to large RNA or DNA substrates.[32] In the present study, in a mouse model with constitutive APOBEC2 expression, nucleotide alterations were induced in RNA sequences of the *Eif4g2* and possibly the *Pten* genes in hepatocytes. Similar to its effect *in vivo*, aberrant APOBEC2 expression in cultured hepatocyte-derived cells induced nucleotide alterations in the *EIF4G2* transcripts. Although our findings demonstrate potential mutator activity of the APOBEC2 protein, it is unclear why the *EIF4G2* transcripts were more sensitive to APOBEC2 activity than other genes in hepatocytes. APOBEC1 expression in hepatocytes also induced somatic mutations in the transcripts of the *EIF4G2* gene.[21] Thus, the sequences of the *EIF4G2* gene might be a common target for the nucleotide editing effects of both the APOBEC1 and APOBEC2 proteins. Further analysis is required to identify the specific target genes of APOBEC2-mediated nucleotide editing in hepatocytes.

An intriguing finding was that the mouse model with constitutive and ubiquitous APOBEC2 expression spontaneously developed epithelial neoplasia in the lung and liver tissues as well as lymphoma. Similar phenotypic findings are observed in mouse models expressing APOBEC1 or AID. Tg mice with RNA-editing enzyme APOBEC1 expression develop HCC at high frequencies with an accumulation of somatic mutations at multiple sites on *Eif4g2* mRNA.[20,21] We also demonstrated that AID Tg mice develop tumors in several organs, including the liver, lung, stomach, and the lymphoid tissues through the accumulation of genetic changes induced by the genotoxic effect of AID.[22,23,28] The molecular mechanisms underlying the contribution of constitutive APOBEC2

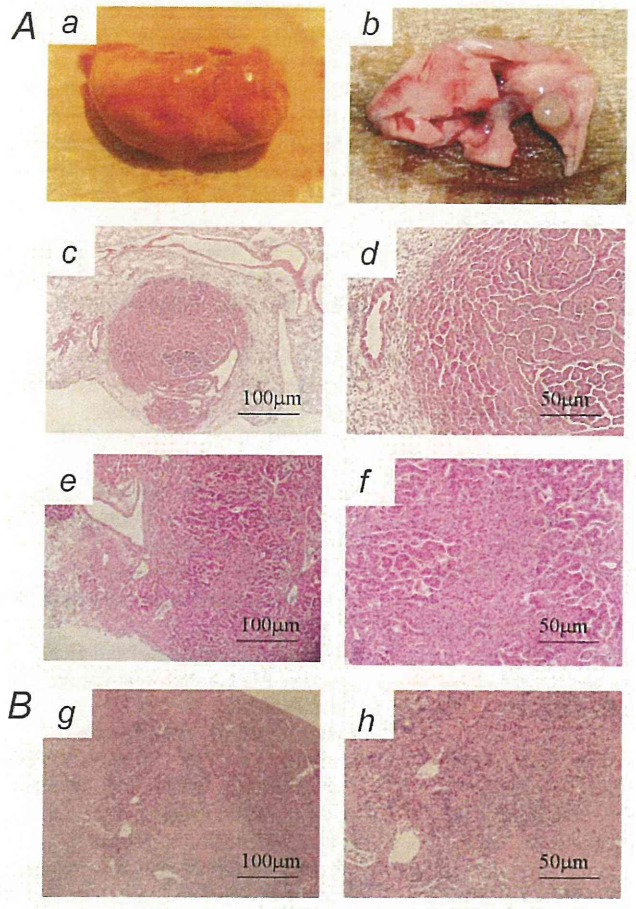

Figure 5. Lung tumors and lymphoma developed in APOBEC2 Tg mice. (*A*) Macroscopic view of a lung tumor that developed in a 72-week-old APOBEC2 Tg mouse (*b*). Microscopic view of a lung adenoma (*c,d*) and adenocarcinoma (*e,f*) that developed in a 72-week-old APOBEC2 Tg mouse. Macroscopic view of the lung of the wild-type littermate (*a*). (*B*) Histologic findings for lymphoma detected in the spleen of APOBEC2 Tg mice. (Original magnifications: 4*c,e,g* ×40; 4*d,f, h* ×100).

expression to tumorigenesis remain unknown. The number of mRNA mutations observed in the *Eif4g2 and Pten* genes in the liver of APOBEC2 Tg mice suggests that these genetic alterations by APOBEC2 have a role in the development of HCC. Indeed, the *EIF4G2* gene is a candidate molecule responsible for oncogenesis caused by the overexpression of APOBEC1,[21] and is frequently downregulated in human cancer tissues.[33] In addition, *PTEN* is one of the most frequently mutated tumor-suppressor genes in human cancers.[34] Thus, the tumorigenesis caused by constitutive APOBEC2 expression might be a consequence of promiscuous nucleotide editing.

Recent studies revealed that the expression of a subset of APOBEC family members is induced by cytokine stimulation in liver tissues. For example, we and other investigators demonstrated that APOBEC3G expression is triggered by interferon-α in hepatocytes, suggesting that APOBEC3G acts as a host defense in response to interferon signaling against viral infection.[35–37] In this study, we showed that TNF-α induced APOBEC2 protein expression in human hepatocytes. Considering the fact that chronic inflammation has important roles in human HCC development,[38,39] the finding that APOBEC2 is induced by proinflammatory cytokine stimulation and induces nucleotide alterations in tumor-related genes in hepatocytes provides a novel idea that aberrant expression of APOBEC2 in epithelial cells acts as a genotoxic factor linking inflammation and cancer development. The tumorigenic phenotype of the APOBEC2-Tg mice further suggests that APOBEC2 is involved in carcinogenesis of the liver tissue under conditions of chronic inflammation, the typical procancerous background of human HCC.

In conclusion, our findings provide the first direct evidence that APOBEC2 induces nucleotide changes preferentially in the *Eif4g2* and possibly the *Pten* genes, and the constitutive expression of APOBEC2 in epithelial tissues contributes to the development of various tumors including HCC and lung cancers. Understanding the pathologic role of APOBEC2 provides new insight into the mechanisms of cancer development in the liver underlying chronic inflammation. During our manuscript preparation, Sato *et al.* reported that they could not find the evidence of APOBEC2's affinity for RNA or high-stoichiometry association with a partner which usually associated with the known RNA editing enzymes.[40] Thus, further analyses would be required to clarify whether APOBEC2 dose possess an RNA-editing activity against specific target genes or overexpression of APOBEC2 causes nucleotide alterations in genome senquences in a promiscuous manner in hepatocytes.

References

1. Wedekind JE, Dance GS, Sowden MP, Smith HC. Messenger RNA editing in mammals: new members of the APOBEC family seeking roles in the family business. *Trends Genet* 2003;19:207–16.
2. Cascalho M. Advantages and disadvantages of cytidine deamination. *J Immunol* 2004; 172:6513–8.
3. Conticello SG, Thomas CJ, Petersen-Mahrt SK, Neuberger MS. Evolution of the AID/APOBEC family of polynucleotide (deoxy)cytidine deaminases. *Mol Biol Evol* 2005;22:367–77.
4. OhAinle M, Kerns JA, Malik HS, Emerman M. Adaptive evolution and antiviral activity of the conserved mammalian cytidine deaminase APOBEC3H. *J Virol* 2006;80:3853–62.
5. Pham P, Bransteitter R, Goodman MF. Reward versus risk: DNA cytidine deaminases triggering immunity and disease. *Biochemistry* 2005;44:2703–15.
6. Chen SH, Habib G, Yang CY, Gu ZW, Lee BR, Weng SA, Silberman SR, Cai SJ, Deslypere JP, Rosseneu M, *et al.* Apolipoprotein B-48 is the product of a messenger RNA with an organ-specific in-frame stop codon. *Science* 1987;238:363–6.
7. Powell LM, Wallis SC, Pease RJ, Edwards YH, Knott TJ, Scott J. A novel form of tissue-specific RNA processing produces apolipoprotein-B48 in intestine. *Cell* 1987; 50:831–40.

8. Mangeat B, Turelli P, Caron G, Friedli M, Perrin L, Trono D. Broad antiretroviral defence by human APOBEC3G through lethal editing of nascent reverse transcripts. *Nature* 2003;424:99–103.
9. Zhang H, Yang B, Pomerantz RJ, Zhang C, Arunachalam SC, Gao L. The cytidine deaminase CEM15 induces hypermutation in newly synthesized HIV-1 DNA. *Nature* 2003;424:94–8.
10. Harris RS, Bishop KN, Sheehy AM, Craig HM, Petersen-Mahrt SK, Watt IN, Neuberger MS, Malim MH. DNA deamination mediates innate immunity to retroviral infection. *Cell* 2003;113:803–9.
11. Shindo K, Takaori-Kondo A, Kobayashi M, Abudu A, Fukunaga K, Uchiyama T. The enzymatic activity of CEM15/Apobec-3G is essential for the regulation of the infectivity of HIV-1 virion but not a sole determinant of its antiviral activity. *J Biol Chem* 2003;278:44412–6.
12. Takaori-Kondo A. APOBEC family proteins: novel antiviral innate immunity. *Int J Hematol* 2006;83:213–6.
13. Noguchi C, Ishino H, Tsuge M, Fujimoto Y, Imamura M, Takahashi S, Chayama K. G to A hypermutation of hepatitis B virus. *Hepatology* 2005;41:626–33.
14. Suspene R, Guetard D, Henry M, Sommer P, Wain-Hobson S, Vartanian JP. Extensive editing of both hepatitis B virus DNA strands by APOBEC3 cytidine deaminases in vitro and in vivo. *Proc Natl Acad Sci USA* 2005;102:8321–6.
15. Noguchi C, Hiraga N, Mori N, Tsuge M, Imamura M, Takahashi S, Fujimoto Y, Ochi H, Abe H, Maekawa T, Yatsuji H, Shirakawa K, *et al.* Dual effect of APOBEC3G on Hepatitis B virus. *J Gen Virol* 2007;88:432–40.
16. Muramatsu M, Sankaranand VS, Anant S, Sugai M, Kinoshita K, Davidson NO, Honjo T. Specific expression of activation-induced cytidine deaminase (AID), a novel member of the RNA-editing deaminase family in germinal center B cells. *J Biol Chem* 1999;274:18470–6.
17. Muramatsu M, Kinoshita K, Fagarasan S, Yamada S, Shinkai Y, Honjo T. Class switch recombination and hypermutation require activation-induced cytidine deaminase (AID), a potential RNA editing enzyme. *Cell* 2000;102:553–63.
18. Liao W, Hong SH, Chan BH, Rudolph FB, Clark SC, Chan L. APOBEC-2, a cardiac- and skeletal muscle-specific member of the cytidine deaminase supergene family. *Biochem Biophys Res Commun* 1999;260:398–404.
19. Mikl MC, Watt IN, Lu M, Reik W, Davies SL, Neuberger MS, Rada C. Mice deficient in APOBEC2 and APOBEC3. *Mol Cell Biol* 2005;25:7270–7.
20. Yamanaka S, Balestra ME, Ferrell LD, Fan J, Arnold KS, Taylor S, Taylor JM, Innerarity TL. Apolipoprotein B mRNA-editing protein induces hepatocellular carcinoma and dysplasia in transgenic animals. *Proc Natl Acad Sci USA* 1995;92:8483–7.
21. Yamanaka S, Poksay KS, Arnold KS, Innerarity TL. A novel translational repressor mRNA is edited extensively in livers containing tumors caused by the transgene expression of the apoB mRNA-editing enzyme. *Genes Dev* 1997;11:321–33.
22. Morisawa T, Marusawa H, Ueda Y, Iwai A, Okazaki IM, Honjo T, Chiba T. Organ-specific profiles of genetic changes in cancers caused by activation-induced cytidine deaminase expression. *Int J Cancer* 2008;123:2735–40.
23. Okazaki IM, Hiai H, Kakazu N, Yamada S, Muramatsu M, Kinoshita K, Honjo T. Constitutive expression of AID leads to tumorigenesis. *J Exp Med* 2003;197:1173–81.
24. Matsumoto T, Marusawa H, Endo Y, Ueda Y, Matsumoto Y, Chiba T. Expression of APOBEC2 is transcriptionally regulated by NF-kappaB in human hepatocytes. *FEBS Lett* 2006;580:731–5.
25. Kou T, Marusawa H, Kinoshita K, Endo Y, Okazaki IM, Ueda Y, Kodama Y, Haga H, Ikai I, Chiba T. Expression of activation-induced cytidine deaminase in human hepatocytes during hepatocarcinogenesis. *Int J Cancer* 2007;120:469–76.
26. Iwai A, Marusawa H, Matsuzawa S, Fukushima T, Hijikata M, Reed JC, Shimotohno K, Chiba T. Siah-1L, a novel transcript variant belonging to the human Siah family of proteins, regulates beta-catenin activity in a p53-dependent manner. *Oncogene* 2004;23:7593–600.
27. Schroeder T, Just U. Notch signalling via RBP-J promotes myeloid differentiation. *Embo J* 2000;19:2558–68.
28. Endo Y, Marusawa H, Kinoshita K, Morisawa T, Sakurai T, Okazaki IM, Watashi K, Shimotohno K, Honjo T, Chiba T. Expression of activation-induced cytidine deaminase in human hepatocytes via NF-kappaB signaling. *Oncogene* 2007;26:5587–95.
29. Doi T, Kinoshita K, Ikegawa M, Muramatsu M, Honjo T. De novo protein synthesis is required for the activation-induced cytidine deaminase function in class-switch recombination. *Proc Natl Acad Sci USA* 2003;100:2634–8.
30. Zhao Y, Pan-Hammarstrom Q, Zhao Z, Hammarstrom L. Identification of the activation-induced cytidine deaminase gene from zebrafish: an evolutionary analysis. *Dev Comp Immunol* 2005;29:61–71.
31. Saunders HL, Magor BG. Cloning and expression of the AID gene in the channel catfish. *Dev Comp Immunol* 2004;28:657–63.
32. Prochnow C, Bransteitter R, Klein MG, Goodman MF, Chen XS. The APOBEC-2 crystal structure and functional implications for the deaminase AID. *Nature* 2007;445:447–51.
33. Buim ME, Soares FA, Sarkis AS, Nagai MA. The transcripts of SFRP1,CEP63 and EIF4G2 genes are frequently downregulated in transitional cell carcinomas of the bladder. *Oncology* 2005;69:445–54.
34. Salmena L, Carracedo A, Pandolfi PP. Tenets of PTEN tumor suppression. *Cell* 2008;133:403–14.
35. Tanaka Y, Marusawa H, Seno H, Matsumoto Y, Ueda Y, Kodama Y, Endo Y, Yamauchi J, Matsumoto T, Takaori-Kondo A, Ikai I, Chiba T. Anti-viral protein APOBEC3G is induced by interferon-alpha stimulation in human hepatocytes. *Biochem Biophys Res Commun* 2006;341:314–9.
36. Bonvin M, Achermann F, Greeve I, Stroka D, Keogh A, Inderbitzin D, Candinas D, Sommer P, Wain-Hobson S, Vartanian JP, Greeve J. Interferon-inducible expression of APOBEC3 editing enzymes in human hepatocytes and inhibition of hepatitis B virus replication. *Hepatology* 2006;43:1364–74.
37. Komohara Y, Yano H, Shichijo S, Shimotohno K, Itoh K, Yamada A. High expression of APOBEC3G in patients infected with hepatitis C virus. *J Mol Histol* 2006;37:327–32.
38. Thorgeirsson SS, Grisham JW. Molecular pathogenesis of human hepatocellular carcinoma. *Nat Genet* 2002;31:339–46.
39. Llovet JM, Burroughs A, Bruix J. Hepatocellular carcinoma. *Lancet* 2003;362:1907–17.
40. Sato Y, Probst HC, Tatsumi R, Ikeuchi Y, Neuberger MS, Rada C. Deficiency in APOBEC2 leads to a shift in muscle fiber-type, diminished body mass and myopathy. *J Biol Chem* 2009;285:7111–18.

OPEN ACCESS Freely available online

PLoS one

Dynamics of Hepatitis B Virus Quasispecies in Association with Nucleos(t)ide Analogue Treatment Determined by Ultra-Deep Sequencing

Norihiro Nishijima[1], Hiroyuki Marusawa[1]*, Yoshihide Ueda[1], Ken Takahashi[1], Akihiro Nasu[1], Yukio Osaki[2], Tadayuki Kou[3], Shujiro Yazumi[3], Takeshi Fujiwara[4], Soken Tsuchiya[4], Kazuharu Shimizu[4], Shinji Uemoto[5], Tsutomu Chiba[1]

1 Department of Gastroenterology and Hepatology, Graduate School of Medicine, Kyoto University, Kyoto, Japan, **2** Department of Gastroenterology and Hepatology, Osaka Red Cross Hospital, Osaka, Japan, **3** Department of Gastroenterology and Hepatology, Tazuke Kofukai Medical Research Institute, Kitano Hospital, Osaka, Japan, **4** Department of Nanobio Drug Discovery, Graduate School of Pharmaceutical Sciences, Kyoto University, Kyoto, Japan, **5** Department of Surgery, Graduate School of Medicine, Kyoto University, Kyoto, Japan

Abstract

Background and Aims: Although the advent of ultra-deep sequencing technology allows for the analysis of heretofore-undetectable minor viral mutants, a limited amount of information is currently available regarding the clinical implications of hepatitis B virus (HBV) genomic heterogeneity.

Methods: To characterize the HBV genetic heterogeneity in association with anti-viral therapy, we performed ultra-deep sequencing of full-genome HBV in the liver and serum of 19 patients with chronic viral infection, including 14 therapy-naïve and 5 nucleos(t)ide analogue(NA)-treated cases.

Results: Most genomic changes observed in viral variants were single base substitutions and were widely distributed throughout the HBV genome. Four of eight (50%) chronic therapy-naïve HBeAg-negative patients showed a relatively low prevalence of the G1896A pre-core (pre-C) mutant in the liver tissues, suggesting that other mutations were involved in their HBeAg seroconversion. Interestingly, liver tissues in 4 of 5 (80%) of the chronic NA-treated anti-HBe-positive cases had extremely low levels of the G1896A pre-C mutant (0.0%, 0.0%, 0.1%, and 1.1%), suggesting the high sensitivity of the G1896A pre-C mutant to NA. Moreover, various abundances of clones resistant to NA were common in both the liver and serum of treatment-naïve patients, and the proportion of M204VI mutants resistant to lamivudine and entecavir expanded in response to entecavir treatment in the serum of 35.7% (5/14) of patients, suggesting the putative risk of developing drug resistance to NA.

Conclusion: Our findings illustrate the strong advantage of deep sequencing on viral genome as a tool for dissecting the pathophysiology of HBV infection.

Citation: Nishijima N, Marusawa H, Ueda Y, Takahashi K, Nasu A, et al. (2012) Dynamics of Hepatitis B Virus Quasispecies in Association with Nucleos(t)ide Analogue Treatment Determined by Ultra-Deep Sequencing. PLoS ONE 7(4): e35052. doi:10.1371/journal.pone.0035052

Editor: Antonio Bertoletti, Singapore Institute for Clinical Sciences, Singapore

Received November 17, 2011; **Accepted** March 8, 2012; **Published** April 16, 2012

Funding: This work was supported by JSPS Grant-in-aid for Scientific Research 21229009, 23390196, and Health and Labor Science Research Grants (H22-08) and Research on Hepatitis from the Ministry of Health, Labor and Welfare, Japan. (http://mhlw-grants.niph.go.jp/). The funders had no role in study design, data collection and analysis, decision to publish, or preparation of the manuscript.

Competing Interests: The authors have declared that no competing interests exist.

* E-mail: maru@kuhp.kyoto-u.ac.jp

Introduction

Hepatitis B virus (HBV) is a non-cytopathic DNA virus that infects approximately 350 million people worldwide and is a main cause of liver-related morbidity and mortality [1–3]. The absence of viral-encoded RNA-dependent DNA polymerase proofreading capacity coupled with the extremely high rate of HBV replication yields the potential to rapidly generate mutations at each nucleotide position within the entire genome [4]. Accordingly, a highly characteristic nature of HBV infection is the remarkable genetic heterogeneity at the inter- and intra- patient level. The latter case of variability as a population of closely-related but nonidentical genomes is referred to as viral quasispecies [5,6]. It is well recognized that such mutations may have important implications regarding the pathogenesis of viral disease. For example, in chronic infection, G to A point mutation at nucleotide (nt) 1896 in the pre-core (pre-C) region as well as A1762T and G1764A mutations in the core-promoter region are highly associated with HBeAg seroconversion that in general results in the low levels of viremia and consequent clinical cure [7–9]. In contrast, acute infection with the G1896A pre-C mutant represents a high risk for fulminant hepatic failure [10,11]. Although these facts clearly illustrate the clinical implications of certain viral mutation, increasing evidence strongly suggests that

the viral genetic heterogeneity is more complicated than previously thought [12,13].

The major goals of antiviral therapy in patients with HBV infection are to prevent the progression of liver disease and inhibit the development of hepatocellular carcinoma [14]. Oral nucleos(t)ide analogue (NA) have revolutionized the management of HBV infection, and five such antiviral drugs, including lamivudine, adefovir, entecavir, tenofovir, and telbivudine, are currently approved medications [15,16]. These agents are well-tolerated, very effective at suppressing viral replication, and safe, but one of the major problems of NA therapy is that long-term use of these drugs frequently causes the emergence of antiviral drug-resistant HBV due to substitutions at specific sites in the viral genome sequences, which often negates the benefits of therapy and is associated with hepatitis flares and death [16,17]. It is unclear whether viral clones with antiviral resistance emerge after the administration of antiviral therapy or widely preexist among treatment-naïve patients.

There has been a recent advance in DNA sequencing technology [18]. The ultra-deep sequencers allow for massively parallel amplification and detection of sequences of hundreds of thousands of individual molecules. We recently demonstrated the usefulness of ultra-deep sequencing technology to unveil the massive genetic heterogeneity of hepatitis C virus (HCV) in association with treatment response to antiviral therapy [19]. On the other hand, there are a few published studies in which this technology was used to characterize genetic HBV sequence variations [20–22]. Margeridon-Thermet et al reported that the 454 Life Science GS20 sequencing platform provided higher sensitivity for detecting drug-resistant HBV mutations in the serum of patients treated with nucleoside and nucleotide reverse-transcriptase inhibitors [20]. Solmone et al also reported the strong advantage conferred by the same platform to detect minor variants in the serum of patients with chronic HBV infection [21]. Although in these previous studies low-abundant drug-resistant variants were successfully detected, the analyses were focused on the reverse-transcriptase region of circulating HBV in the serum and thus the whole picture of HBV genetic heterogeneity as well as the *in vivo* dynamics of HBV drug resistant variants in response to anti-viral treatment remains to be clarified. Moreover, intrahepatic viral heterogeneity in patients that achieved the clearance of circulating HBV is largely unknown.

By taking the advantage of an abundance of genetic information obtained by utilizing the Illumina Genome Analyzer II (Illumina, San Diego, CA) as a platform of ultra-deep sequencing, we determined the whole HBV sequence in the liver and serum of patients with chronic HBV infection to evaluate viral quasispecies characteristics. Moreover, we investigated the prevalence of rare drug-resistant HBV variants as well as detailed dynamic changes in the viral genetic heterogeneity in association with NA administration. Based on the abundant genetic information obtained by ultra-deep sequencing, we clarified the precise prevalence of HBV clones with G1896A pre-C mutations in association with HBe serostatus in chronically infected patients with or without NA treatment. We also detected a variety of minor drug-resistant clones in treatment-naïve patients and their dynamic changes in response to entecavir administration, demonstrating the potential clinical significance of naturally-occurring drug-resistant mutations.

Materials and Methods

Ethics Statement

The Kyoto University ethics committee approved the study, and written informed consent for participation in this study was obtained from all patients. The study was conducted in accordance with the principles of the Declaration of Helsinki.

Patients

The liver tissues of 19 Japanese patients that underwent living-donor liver transplantation at Kyoto University due to HBV-related liver disease were available for viral genome analyses. These individuals included 13 men and 6 women, aged 41 to 69 years (median, 55.2 years) and all but one were infected with genotype C viruses. Participants comprised 19 patients with liver cirrhosis caused by chronic HBV infection, including 14 antiviral therapy-naïve cases (chronic-naïve cases) and 5 cases receiving NA treatment, with either lamivudine or entecavir (chronic-NA cases) (Table 1). Serum HBV DNA levels were significantly higher in chronic-naïve cases than in chronic NA cases (median serum HBV DNA levels were 5.6, and <2.6 log copies/ml, respectively, Table 1). Liver tissue samples were obtained at the time of transplantation, frozen immediately, and stored at $-80°C$ until use. Serologic analyses of HBV markers, including hepatitis B surface antigen (HBsAg), antibodies to HBsAg, anti-HBc, HBeAg, and antibodies to HBeAg, were determined by enzyme immunoassay kits as described previously [23]. HBV DNA in the serum before transplantation was examined using a polymerase chain reaction (PCR) assay (Amplicor HBV Monitor, Roche, Branchburg, NJ). To examine the dynamics of viral quasispecies in response to anti-HBV therapy, paired serum samples of 14 treatment-naïve patients before and after administration of daily entecavir (0.5 mg/day) were subjected to further analyses on viral genome.

Direct population Sanger sequencing

DNA was extracted from the liver tissue and serum using a DNeasy Blood & Tissue Kit (Qiagen, Tokyo, Japan). To define the consensus reference sequences of HBV in each clinical specimen, all samples were first subjected to direct population Sanger sequencing using the Applied Biosystems 3500 Genetic Analyzer (Applied Biosystems, Foster City, CA). Oligonucleotide primers for the HBV genome were designed to specifically amplify whole viral sequences as two overlapping fragments using the sense primer 169_F and antisense primer 2847_R to yield a 2679-bp amplicon (amplicon 1), and the sense primer 685_F and antisense primer 443_R to yield a 2974-bp amplicon (amplicon 2; Table S1). HBV sequences were amplified using Phusion High-Fidelity DNA polymerase (FINZYMES, Espoo, Finland). All amplified PCR products were purified using the QIAquick Gel Extraction kit (Qiagen) after agarose gel electrophoresis and used for direct sequencing. The serum of a healthy HBV DNA-negative volunteer was used as a negative control.

Viral genome sequencing by massively-parallel sequencing

Massively-parallel sequencing with multiplexed tags was performed using the Illumina Genome Analyzer II as described [19]. The end-repair of DNA fragments, addition of adenine to the 3′ ends of DNA fragments, adaptor ligation, and PCR amplification by Illumina PCR primers were performed as described previously [24]. Briefly, the viral genome sequences were amplified by high-fidelity PCR using oligonucleotide primers as described above, sheared by nebulization using 32 psi N2 for 8 min, and then the sheared fragments were purified and concentrated using a QIAquick PCR purification Kit (Qiagen). Nucleotide overhangs resulting from fragmentation were then converted into blunt ends using T4 DNA polymerase and Klenow

Table 1. Characteristics of patients with chronic HBV infection analyzed in this study.

	Chronic-naïve (N = 14)	Chronic-NA (N = 5)
Age†	55.5 (41–69)	55.0 (49–68)
Sex (male/female)	9/5	4/1
Alanine aminotransaminase (IU/l)†	41 (10–74)	30 (15–65)
Total bilirubin (mg/dl)†	0.9 (0.5–31.1)	1.7 (0.6–4.5)
Platelet count ($\times 10^4/mm^3$)†	12.7 (3.3–27.6)	5.1 (3.6–11.3)
HBV genotype		
B	1	0
C	13	5
Viral load (log copies /ml)†	5.6 (<2.6–8.8)*	<2.6 (<2.6–5.3)*
HBe-serostatus (HBeAg+/HBeAb+)	8/6	0/5
Fibrosis		
F0–F2	6	0
F3–F4	8	5
Activity		
A0–A1	7	3
A2–A3	7	2

†Values are median (range).
*P = 0.042.
doi:10.1371/journal.pone.0035052.t001

enzymes, followed by the addition of terminal 3′ A-residues. An adaptor containing unique 6-bp tags, such as "ATCACG" and "CGATGT" (Multiplexing Sample Preparation Oligonucleotide Kit, Illumina), was then ligated to each fragment using DNA ligase. We then performed agarose gel electrophoresis of adaptor-ligated DNAs and excised bands from the gel to produce libraries with insert sizes ranging from 200 to 350 bp. These libraries were amplified independently using a minimal PCR amplification step of 18 cycles by Illumina PCR primers with Phusion High-Fidelity DNA polymerase. The DNA fragments were then purified with a MinElute PCR Purification Kit (Qiagen), followed by quantification using the NanoDrop 2000C (Thermo Fisher Scientific, Waltham, MA) to make a working concentration of 10 nM. Cluster generation and sequencing was performed for 64 cycles on the Illumina Genome Analyzer II according to the manufacturer's instructions. The obtained images were analyzed and base-called using GA pipeline software version 1.4 with the default settings provided by Illumina.

Genome Analyzer sequence data analysis

Using the high performance alignment software "NextGene" (SoftGenetics, State College, PA), the 64 base-pair reads obtained from the Genome Analyzer II were aligned with the reference sequences of 3215 bp that were determined by direct population Sanger sequencing of each clinical specimen. Reads with 90% or more bases matching a particular position of the reference sequences were aligned. Furthermore, two quality filters were used for sequencing reads: the reads with a median quality score of more than 30 and no more than 3 uncalled nucleotides were allowed anywhere in the 64 bases. Only sequences that passed the quality filters, rather than raw sequences, were analyzed and each position of the viral genome was assigned a coverage depth, representing the number of times the nucleotide position was sequenced.

Allele-specific quantitative real-time PCR and semiquantitative PCR to determine the relative proportion of G1896A pre-C mutant

To determine the relative proportion of the G1896A pre-C mutant, allele-specific quantitative real-time PCR was performed based on the previously described method [25,26]. Oligonucleotide primers were designed individually to amplify the pre-C region of wild-type and the G1896A pre-C mutant HBV. Three primers were used for this protocol, two allele-specific sense primers, 1896WT_F (for wild-type) and 1896MT_F (for the G1896A pre-C mutant), and one common antisense primer, 2037_R (Table S1). Quantification of wild-type and the G1896A pre-C mutant was individually performed by real-time PCR using a Light Cycler 480 and Fast Start Universal SYBR Master (Roche, Mannheim, Germany) [27]. The relative proportion of the G1896A pre-C mutant was determined to calculate the G1896A pre-C mutant/total HBV ratios. Performance of this assay was tested using mixtures of two previously described plasmids, pcDNA3-HBV-wt#1 and pcDNA3-HBV-G1896A pre-C mutant [28]. Semiquantitative PCR was performed using primers described above, then agarose gel electrophoresis was performed.

Statistical analysis

Results are expressed as mean or median, and range. Pretreatment values were compared using the Mann-Whitney U-test or the Kruskal Wallis H-test. *P* values less than 0.05 were considered statistically significant.

The viral quasispecies characteristics were evaluated by analyzing the genetic complexity based on the number of different sequences present in the population. Genetic complexity for each site was determined by calculating the Shannon entropy using the following formula:

$$Sn = -\frac{\sum_{i=1}^{n} fi(lnfi)}{N}$$

where n is the number of different species identified, fi is the observed frequency of a particular variant in the quasispecies, and N is the total number of clones analyzed [12,13]. The mean viral complexity in each sample was determined by calculating the total amounts of the Shannon entropy at each nucleotide position divided by the total nucleotide number (e.g., 3215 bases) of each HBV genome sequence.

Nucleotide sequence accession number

All sequence reads have been deposit in DNA Data Bank of Japan Sequence Read Archive (http://www.ddbj.nig.ac.jp/index-e.html) under accession number DRA000435.

Results

Validation of multiplex ultra-deep sequencing of the HBV genome

To differentiate true mutations from sequencing errors in the determined sequences, we first generated viral sequence data from the expression plasmid, pcDNA3-HBV-wt#1, encoding wild-type genotype C HBV genome sequences [28]. For this purpose, we determined the PCR-amplified HBV sequences derived from the expression plasmid using high-fidelity Taq polymerase to take the PCR-induced errors as well as sequencing errors into consideration. Viral sequences determined by the conventional Sanger method were used as reference sequences for aligning the amplicons obtained by ultra-deep sequencing. Three repeated ultra-deep sequencing generated a mean of 77,663 filtered reads, corresponding to a mean coverage of 38,234 fold at each nucleotide site (Table S2). Errors comprised insertions (0.00003%), deletions (0.00135%), and nucleotide mismatches (0.037%). The mean overall error rate was 0.034% (distribution of per-nucleotide error rate ranged from 0 to 0.13%) for the three control experiments, reflecting the error introduced by high-fidelity PCR amplification and by multiplex ultra-deep sequencing that remained after filtering out problematic sequences. We also confirmed that multiplex ultra-deep sequencing with and without the high-fidelity PCR amplification with HBV-specific primer sets showed no significant differences in the error rates on the viral sequence data (mean error rate 0.034% vs 0.043%). Accordingly, we defined the cut-off value in its current platform as 0.3%, a value nearly 1 log above the mean overall error rate.

Next, we performed additional control experiments to verify the detectability of the low abundant mutations that presented at a frequency of less than 0.3%. For this purpose, we introduced expression plasmids with a single-point mutation within that encoding a wild-type viral sequence with a ratio of 1:1000 and assessed the sensitivity and accuracy of quantification using high-fidelity PCR amplification followed by multiplex ultra-deep sequencing in association with the different coverage numbers (Table S3). Repeated control experiments revealed that the threshold for detecting low-abundant mutations at an input ratio of 0.10% among the wild-type sequences ranged between 0.11% and 0.24%, indicating that there was no significant difference in the detection rate or error rates under the different coverage conditions. Based on these results, the accuracy of ultra-deep sequencing in its current platform for detecting low-level viral mutations was considered to be greater than 0.30%.

Viral complexity of the HBV quasispecies in association with clinical status

To clarify HBV quasispecies in association with clinical status, we performed multiplex ultra-deep sequencing and determined the HBV full-genome sequences in the liver and serum with chronic HBV infection. First, we compared the sequences of the viral genome determined in the liver tissue with those in the serum and found no significant differences in the viral population between the liver and serum of the same individual. Indeed, the pattern and distribution of genetic heterogeneity of the viral nucleotide sequences in the liver tissue were similar to those observed in the serum of the same patient (Figure S1), suggesting that a similar pattern of viral heterogeneity was maintained in the liver and serum of patients with chronic HBV infection.

Next, we compared the viral heterogeneity in the liver of chronic-naïve and chronic-NA cases. A mean of 5,962,996 bp nucleotides in chronic-naïve cases and 4,866,783 bp nucleotides in chronic-NA cases were mapped onto the reference sequences, and an overall average coverage depth of 1,855 and 1.514 was achieved for each nucleotide site of the HBV sequences, respectively (Table 2). The frequencies of mutated positions and altered sequence variations detected in each viral genomic region are summarized in Table 2. The overall mutation frequency of the total viral genomic sequences was determined to be 0.87% in chronic-naïve cases and 0.69% in chronic-NA cases. Most genomic changes observed in viral variants were single base substitutions, and the genetic heterogeneity of the viral nucleotide sequences was equally observed throughout the individual viral genetic regions, including the pre-surface (preS), S, pre-core~core (preC-C), and X (Table 2). Consistent with the findings obtained from the viral mutation analyses, the overall viral complexity determined by the Shannon entropy value was 0.047 in chronic-naïve and 0.036 in chronic-NA cases, and the viral complexity was equally observed throughout the individual viral genetic region (Figure 1A). Among chronic-naïve cases, we observed no significant differences in the viral complexity in HBV DNA level, age, or degree of fibrosis (Figure 1B).

High sensitivity of the G1896A pre-C mutant to nucleos(t)ide analogues

Emergence of G1896A mutation in the pre-C region, and A1762T and G1764A mutations in the core-promoter region is well known to be associated with HBe-seroconversion [7–9]. We then evaluated the prevalence of these three mutations in the chronically HBV-infected liver, in association with HBe serologic status and the NA treatment history. In chronic-naive cases, 6 and 8 patients showed the pre- and post- HBeAg seroconversion status, respectively (Table 3). The mean prevalence of the G1896A pre-C mutant in HBeAg-positive cases was lower than that in the HBeAg-negative cases (27.4% and 46.5%, respectively). Importantly, however, 4 of 8 HBeAg-negative cases showed a relatively low prevalence of the G1896A pre-C mutant (Liver #8, #12, #13, #14), and all but one case (Liver #10) showed a high prevalence of the A1762T and G1764A mutations, irrespective of HBe serologic status and NA treatment history (Table 3). These findings suggested that other mutations except G1896A, A1762T and G1764A were also involved in the HBeAg seroconversion status. Notably, liver tissues of all but one (Liver #17) chronic-NA cases showed extremely low levels of the G1896A pre-C mutant (0.0, 0.0, 0.1, and 1.1%), suggesting the high sensitivity of the G1896A pre-C mutant to NA (Table 3).

To confirm the difference of the sensitivity to NA between the wild-type and the G1896A pre-C mutant, we examined the dynamic changes of the relative proportion of the G1896A pre-C mutant in the serum of 14 treatment-naïve patients before and after entecavir administration. Consistent with the findings obtained by ultra-deep sequencing, quantitative real-time PCR revealed that entecavir administration significantly reduced the proportion of the G1896A pre-C mutant in 13 of 14 cases (92.9%)

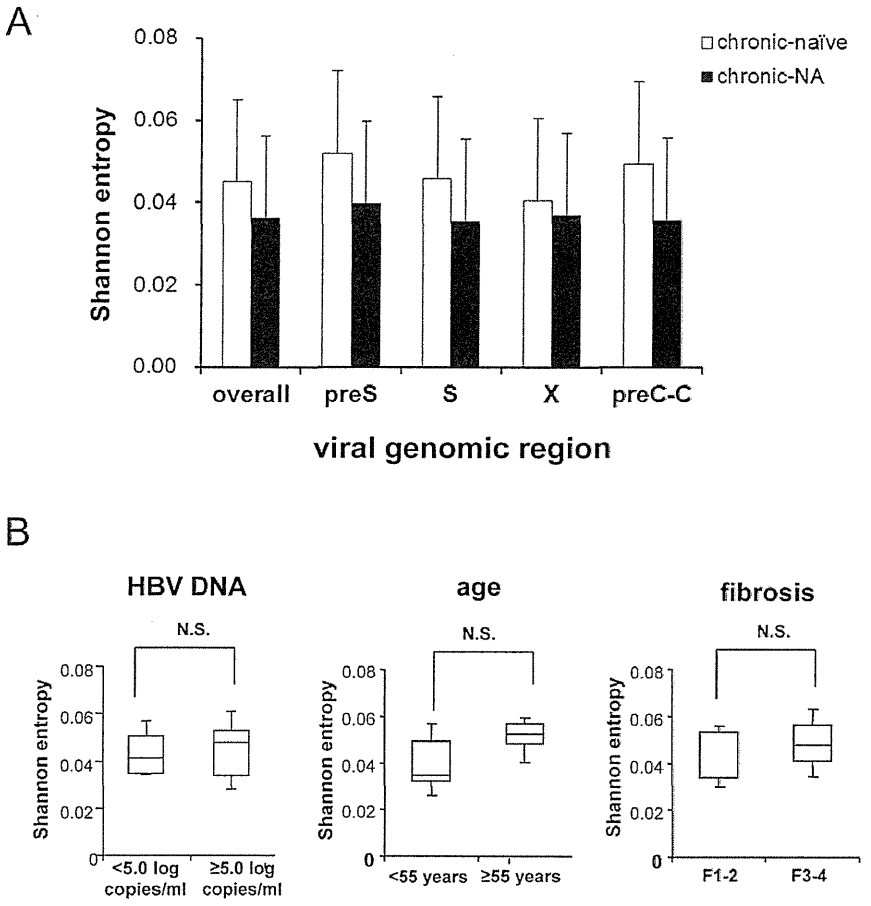

Figure 1. Viral complexity of the HBV quasispecies in association with clinical status. (A) The Shannon entropy values for each viral genomic region were determined in the liver of chronic-naïve and chronic-NA cases. (B) Among the chronic-naïve cases, the Shannon entropy values are shown for patients with serum HBV DNA levels less than 5.0 log copies/ml (<5.0) and greater than 5.0 log copies/ml (≥5.0) (left panel), patients under the age of 55 years (<55) and over the age of 55 (≥55) (middle panel), and patients with low (F1–2) and high (F3–4) liver fibrosis levels (right panel). preS: pre-surface, preC-C: precore~core N.S.: not significant.
doi:10.1371/journal.pone.0035052.g001

Table 2. The frequency of mutation rate and the Shannon entropy in each viral genome region.

	Liver	
	Chronic-naïve (N = 14)	**Chronic-NA (N = 5)**
Average aligned reads	93,172	76,043
Average aligned nucleotides	5,962,996	4,866,783
Average coverage	1,855	1,514
Mutation rate (%)		
Overall	0.87	0.69
preS	0.92	0.81
S	0.96	0.71
preC-C	1.05	0.72
X	0.63	0.61
Shannon entropy	0.047	0.036

Mutation rate (%): the ratio of total different nucleotides from the reference sequence to total aligned nucleotides.
preS: pre-surface, preC-C: pre-core~core.
doi:10.1371/journal.pone.0035052.t002

irrespective of their HBeAg serostatus, while the G1896A pre-C mutant were detectable in substantial proportion before treatment in all cases (Figure 2A, 2B and 2C; $p = 0.001$). These results further support the findings that HBV clones comprising the G1896A mutation were more sensitive to NA than those with wild-type sequences.

Prevalence of drug-resistant HBV clones in the liver of treatment-naïve patients

Increasing evidence suggests that drug-resistant viral mutants can be detected in the serum of treatment-naïve patients with chronic HBV infection [20,21]. Thus, we next determined the actual prevalence of spontaneously-developed drug-resistant mutants in chronically-infected liver of treatment-naïve patients to evaluate whether NA treatment potentiates the expansion of drug-resistant clones. The drug-resistant mutations examined included two mutations resistant to lamivudine and entecavir, four mutations resistant to entecavir, and three mutations resistant to adefovir [16,17]. Based on the detection rate of the low-level viral clones determined by the control experiments, we identified the drug-resistant mutants present in each specimen at a frequency of more than 0.3% among the total viral clones. Based on these criteria, at least one resistant mutation was detected in the liver of all of the chronic-naïve cases with chronic HBV infection (Table 4).